

Comprehensive *In Vitro* Analysis of Simian Retrovirus Type 4 Susceptibility to Antiretroviral Agents

Hiroaki Togami,^a Kazuya Shimura,^a Munehiro Okamoto,^b Rokusuke Yoshikawa,^c Takayuki Miyazawa,^c Masao Matsuoka^a

Laboratory of Virus Control, Institute for Virus Research, Kyoto University, Kyoto, Japan^a; Section of Wildlife Diversity, Center for Human Evolution Modeling Research, Primate Research Institute, Kyoto University, Inuyama, Japan^b; Laboratory of Signal Transduction, Institute for Virus Research, Kyoto University, Kyoto, Japan^c

Simian retrovirus type 4 (SRV-4), a simian type D retrovirus, naturally infects cynomolgus monkeys, usually without apparent symptoms. However, some infected monkeys presented with an immunosuppressive syndrome resembling that induced by simian immunodeficiency virus infection. Antiretrovirals with inhibitory activity against SRV-4 are considered to be promising agents to combat SRV-4 infection. However, although some antiretrovirals have been reported to have inhibitory activity against SRV-1 and SRV-2, inhibitors with anti-SRV-4 activity have not yet been studied. In this study, we identified antiretroviral agents with anti-SRV-4 activity from a panel of anti-human immunodeficiency virus (HIV) drugs using a robust *in vitro* luciferase reporter assay. Among these, two HIV reverse transcriptase inhibitors, zidovudine (AZT) and tenofovir disoproxil fumarate (TDF), potently inhibited SRV-4 infection within a submicromolar to nanomolar range, which was similar to or higher than the activities against HIV-1, Moloney murine leukemia virus, and feline immunodeficiency virus. In contrast, nonnucleoside reverse transcriptase inhibitors and protease inhibitors did not exhibit any activities against SRV-4. Although both AZT and TDF effectively inhibited cell-free SRV-4 transmission, they exhibited only partial inhibitory activities against cell-to-cell transmission. Importantly, one HIV integrase strand transfer inhibitor, raltegravir (RAL), potently inhibited single-round infection as well as cell-free and cell-to-cell SRV-4 transmission. These findings indicate that viral expansion routes impact the inhibitory activity of antiretrovirals against SRV-4, while only RAL is effective in suppressing both the initial SRV-4 infection and subsequent SRV-4 replication.

Simian type D retroviruses (SRV/Ds) are prevalent among wild and colony-born macaque monkeys, including *Macaca fascicularis* (cynomolgus) and *M. mulatta* (rhesus) (1–3). Although SRV/D infection is asymptomatic in most of these monkeys, mild immunosuppression accompanied by anemia, diarrhea, and splenomegaly has been observed in infected cynomolgus monkeys (3, 4). Recently, Japanese macaques (*M. fuscata*) housed in the Primate Research Institute (PRI) of Kyoto University, Japan, died of a hemorrhagic syndrome with symptoms such as anorexia, pallor, and nasal hemorrhage (5). Extensive investigations revealed that this illness was caused by an infection with an SRV/D known as simian retrovirus type 4 (SRV-4) (5; M. Okamoto et al., unpublished data). SRV-4 has been reported to be distantly related to other SRV/Ds, including SRV-1, -2, -3, -5, -6, and -7; e.g., the previously isolated SRV-4 showed genome sequence similarities of 78, 76, and 74% to SRV-1, -2, and -3, respectively (6). Although there is more than 80% amino acid sequence identity between Gag, Prt, and Pol of SRV-4 and SRV-1, -2, or -3, the Env sequence of SRV-4 is relatively diverse (67 to 74%) compared to other SRV/Ds (6). Although SRV-4 asymptotically infects cynomolgus monkeys (7), SRV-4 infection of Japanese macaques has not been reported to date. Because the cause of the high mortality observed only for SRV-4-infected Japanese monkeys at PRI remains unclear, it is important to study SRV-4 pathogenesis in Japanese monkeys and to develop a prevention/treatment strategy for controlling SRV-4 infection.

Human immunodeficiency virus (HIV) infection remains a significant threat to humans. Over 20 antiviral drugs have been approved for the treatment of HIV-1-infected individuals. Antiretroviral therapy (ART) can efficiently suppress viral load and enable the recovery of immune function in HIV-1-infected individuals. Some of these drugs suppress infections caused by other

retroviruses, including murine leukemia virus (MLV) (8, 9), xenotropic murine leukemia-related retrovirus (XMRV) (10, 11), feline immunodeficiency virus (FIV) (12, 13), and human T-cell leukemia virus type 1 (HTLV-1) (14, 15), indicating that some anti-HIV drugs are widely active against several other retroviruses. There have been some reports on the anti-SRV/D activity of anti-HIV drugs. Tsai et al. reported that three nucleoside/nucleotide reverse transcriptase inhibitors (NRTIs), zidovudine (AZT), zalcitabine (ddC), and 2',3'-deoxyadenosine (ddA), exhibited inhibitory activity against SRV-2 infection *in vitro* (16). Moreover, although ddC treatment induced no major change in viral titers in pigtailed monkeys (*M. nemestrina*) naturally infected with SRV-2, the prophylactic use of ddC blocked *de novo* SRV-2 infection in this species (17). Rosenblum et al. reported that anti-SRV-1 and anti-SRV-2 activities of several NRTIs were relatively comparable with anti-HIV-1 activity (18). Furthermore, elvitegravir (EVG) and raltegravir (RAL), which are HIV-1 integrase strand transfer inhibitors (INSTIs), efficiently block SRV-3 (also known as Mason-Pfizer monkey virus) infection at nanomolar concentrations (19). Thus, some NRTIs and INSTIs exhibit anti-SRV/D activity; however, whether these drugs are active against SRV-4 infection remains unclear.

In this study, we extensively evaluated the anti-SRV-4 activity of a series of anti-HIV inhibitors, including NRTIs, nonnucleo-

Received 16 November 2012 Accepted 25 January 2013

Published ahead of print 30 January 2013

Address correspondence to Kazuya Shimura, kshimura@virus.kyoto-u.ac.jp.

Copyright © 2013, American Society for Microbiology. All Rights Reserved.

doi:10.1128/JVI.03208-12

side reverse transcriptase inhibitors (NNRTIs), an INSTI, and protease inhibitors (PIs), *in vitro* using single-round infection and multiround viral spread by cell-free and cell-to-cell transmission. Among the NRTIs tested, AZT and tenofovir disoproxil fumarate (TDF) efficiently blocked single-round infection and cell-free transmission of SRV-4, although they were less effective against cell-to-cell transmission. RAL, an INSTI, blocked single-round infection and cell-free transmission of SRV-4 within the nanomolar range, and notably, it was also effective against cell-to-cell SRV-4 transmission. These results indicate that AZT, TDF, and RAL are effective in blocking the initial SRV-4 infection, and particularly, RAL is the most promising drug for the control of SRV-4 replication.

MATERIALS AND METHODS

Antiviral agents. Didanosine (ddI) (NRTI), lamivudine (3TC) (NRTI), stavudine (d4T) (NRTI), ddC (NRTI), AZT (NRTI), and nelfinavir (NFV) (PI) were purchased from Sigma (St. Louis, MO). Efavirenz (EFV) (NNRTI), nevirapine (NVP) (NNRTI), and saquinavir (SQV) (PI) were purchased from Toronto Research Chemicals (Ontario, Canada). Emtricitabine (FTC) (NRTI), TDF (NRTI), darunavir (DRV) (PI), and RAL (INSTI) were obtained through the AIDS Research and Reference Reagent Program, National Institute of Allergy and Infectious Diseases (NIAID), National Institutes of Health (NIH).

Cells and viruses. TE671 (human rhabdomyosarcoma), 293T (human embryonic kidney), and 293T/SRV-4 (a persistently SRV-4-infected 293T cell line) cells, which have been established by the transfection of an SRV-4 infectious clone into 293T cells (Okamoto et al., unpublished), were grown in Dulbecco's modified Eagle's medium (DMEM). MT-2 cells (human T lymphocytes) were grown in RPMI 1640 medium. These media were supplemented with 10% fetal calf serum (FCS), 2 mM L-glutamine, 100 U/ml penicillin, and 50 µg/ml streptomycin. 293FT cells (Invitrogen, Carlsbad, CA) were cultured in DMEM supplemented with 0.5 mg/ml G418. Platinum-GP cells (Plat-GP; Cell Biolabs, San Diego, CA) were maintained in DMEM supplemented with 10 µg/ml blasticidin.

Concentrated SRV-4 was prepared as follows: 293T/SRV-4 cells (10^6 cells) were cultured in a T-75 flask. After 3 days, culture supernatants were recovered and filtered through a 0.45-µm membrane, followed by the addition of a 30% polyethylene glycol (PEG) solution and 1.2 M sodium chloride. The mixture was then incubated overnight at 4°C, followed by centrifugation at 3,000 rpm for 45 min at 4°C. The resultant pellet was resuspended in DMEM and used for assays immediately after titration.

Quantification of the proviral copy number. Viral RNA and genomic DNA were prepared from concentrated SRV-4 by using the QIAamp viral RNA minikit (Qiagen, Hilden, Germany) and from SRV-4-infected 293T cells by using DNAzol (Invitrogen), respectively. The viral copy number was quantified by using the One Step PrimeScript reverse transcriptase PCR (RT-PCR) kit (TaKaRa, Otsu, Japan) and the StepOnePlus real-time PCR system (Applied Biosystems, Foster City, CA) with a known copy number control. The primer sets and a probe used for SRV-4 amplification were described previously (20). PCR conditions were 5 min at 42°C, 10 s at 95°C, and 55 cycles of 5 s at 95°C and 34 s at 62°C.

VSV-G-pseudotyped luciferase expression vectors. An envelope-deleted SRV-4-based firefly luciferase expression vector, Δenv-SRV-4-luc (R. Yoshikawa et al., unpublished data), and a plasmid, pcDNA-VSV-G, encoding the vesicular stomatitis virus envelope glycoprotein (VSV-G) (provided by H. Miyoshi, Riken Bioresource Center, Tsukuba, Japan) were used to generate VSV-G-pseudotyped luciferase-expressing SRV-4. These plasmids were cotransfected into 293FT cells. After 48 h of transfection, culture supernatants were recovered, filtered through a 0.45-µm membrane, and stored at -80°C until use.

The VSV-G-pseudotyped luciferase-expressing HIV-1-based lentiviral vector was generated as reported previously (9). The Moloney MLV (MoMLV)-based retroviral vector was produced by cotransfection of the

pDON-AI-2-luc plasmid, a firefly luciferase gene-containing pDON-AI-2 retroviral vector (TaKaRa) (provided by Y. Sakurai, Institute for Virus Research, Kyoto University, Kyoto, Japan), and pcDNA-VSV-G into a MoMLV-based packaging cell line, Plat-GP. The FIV-based lentiviral vector was prepared by cotransfection of a luciferase-encoding transfer vector, pCDF-luc-EF1-puro; a 34TF10-derived packaging vector, pFIV-34N (SBI System Biosciences, Mountain View, CA); and pcDNA-VSV-G into 293FT cells. All the recombinant viruses were collected and stored as mentioned above.

Evaluation of the anti-SRV-4 activities of NRTIs, NNRTIs, and an INSTI in single-round infection. To evaluate the inhibitory activities of anti-HIV drugs against VSV-G-pseudotyped luciferase-expressing SRV-4, HIV-1, MoMLV, and FIV, TE671 cells (10^4 cells/well) were plated onto white 96-well flat plates. After 24 h of incubation, the cells were infected with each virus in the presence of various concentrations of inhibitors. Similarly, 3×10^5 MT-2 cells were infected separately. Luciferase activity was determined by using the Bright-Glo luciferase assay system (Promega, Madison, WI) and a TriStar LB 941 multimode microplate reader (Berthold, Bad Wildbad, Germany) at 48 h postinfection. Cytotoxicity of the inhibitors was measured by using the 3-(4,5-dimethylthiazol-2-yl)-2,5-diphenyltetrazolium bromide (MTT) colorimetric assay, as described previously (9). Antiviral activity and cytotoxicity of the inhibitors are presented as the concentration that blocks viral infection by 50% (50% effective concentration [EC₅₀]) and the concentration that inhibits cell viability by 50% (50% cytotoxic concentration [CC₅₀]), respectively.

Evaluation of the inhibitory activity of PI against SRV-4 production. 293T/SRV-4 cells were washed three times with phosphate-buffered saline (PBS) and plated at a density of 2×10^5 cells/well onto a six-well culture plate in the presence of various concentrations of PIs. After 72 h of incubation, culture supernatants were collected and concentrated as described above. The resultant pellet was solubilized with lysis buffer supplied in the Reverse Transcriptase Assay, colorimetric (Roche, Mannheim, Germany), and RT activity was quantified to evaluate viral production.

Effects of AZT, TDF, and RAL on SRV-4 replication. To test cell-free SRV-4 infection, 293T cells were plated at a density of 2×10^5 cells/well onto a six-well plate and pretreated with inhibitors of approximately $10 \times$ EC₅₀s determined by the single-round luciferase assay (AZT [400 nM], TDF [10 nM], and RAL [150 nM]) or dimethyl sulfoxide (DMSO) as a control for 4 h. Following this, culture media were replaced with fresh medium containing identical concentrations of each inhibitor, and the cells were infected with concentrated (37.5-fold) replication-competent SRV-4 at a multiplicity of infection (MOI) of 2.0×10^6 copies/cell.

For cell-to-cell SRV-4 infection, SRV-4-free 293T cells (2×10^5 cells) were pretreated with inhibitors as described above for the cell-free infection assay. Following this, 293T/SRV-4 cells (4×10^3 cells; proviral copy number, $5 \times 10^{1.3}$ copies/cell) were cocultured in the presence of identical concentrations of inhibitors.

In both the experimental approaches, culture supernatants were collected and replenished with an equal volume of fresh medium containing the corresponding inhibitors on days 1, 3, and 5 postinfection/postcoculture. SRV-4 in each collected supernatant was concentrated, and RT activity was quantified to monitor viral replication.

Statistical analysis. Dunnett's test and the Bonferroni test were used to determine the statistical significance of anti-SRV-4 activity of inhibitors in single-round assays (Table 1) and of SRV-4 transmission in cell-free and cell-to-cell infection assays (Fig. 1), respectively.

Protein sequence alignment. Standard amino acid sequences of SRV-4 (GenBank accession number NC_014474.1), HIV-1 (accession number NC_001802.1), MoMLV (accession number NC_001501.1), and FIV (accession number NC_001482.1) were aligned by using the program Clustal W (21), as described previously (9). Residues associated with drug resistance in HIV-1, reported in the Stanford University HIV Drug Resistance Database (22), are also shown.

TABLE 1 Susceptibility of VSV-G-pseudotyped luciferase-expressing SRV-4 and related retroviruses/lentiviruses to NRTIs and an INSTI in single-round infection^a

Target cell line and inhibitor	Mean EC ₅₀ ± SD (μM) (mean % inhibition ± SD)			
	HIV-1	SRV-4	MoMLV	FIV
TE671				
NRTIs				
Thymidine analogs				
AZT	0.018 ± 0.0074	0.042 ± 0.012*	0.019 ± 0.0043	0.029 ± 0.0035
d4T	0.40 ± 0.10	0.17 ± 0.039	3.7 ± 0.82**	0.52 ± 0.0055
Inosine analog				
ddI	10 ± 1.7	4.4 ± 1.3**	>10 (0)	19 ± 1.7**
Cytidine analogs				
ddC	5.6 ± 1.1	2.7 ± 0.13**	>10 (0)**	3.2 ± 0.50**
3TC	4.4 ± 0.75	3.9 ± 1.2	>10 (0)**	2.2 ± 0.50*
FTC	0.48 ± 0.15	0.50 ± 0.082	>10 (0)**	0.35 ± 0.030
Adenosine analog				
TDF	0.0043 ± 0.00058	0.00080 ± 0.00037**	0.0035 ± 0.0012	0.0015 ± 0.00076**
INSTI				
RAL	0.0031 ± 0.0015	0.015 ± 0.0065	0.0017 ± 0.00036	0.049 ± 0.00090*
MT-2				
NRTIs				
Thymidine analogs				
AZT	0.037 ± 0.014	0.11 ± 0.037	0.71 ± 0.36*	1.4 ± 0.40**
d4T	0.50 ± 0.13	2.3 ± 0.44	3.5 ± 0.61	21 ± 6.6**
Inosine analog				
ddI	3.4 ± 0.70	>10 (42 ± 4.4)*	>10 (0)*	16 ± 4.7**
Cytidine analogs				
ddC	7.2 ± 2.4	0.59 ± 0.45**	>10 (0)	3.5 ± 1.1*
3TC	2.8 ± 1.0	>10 (17 ± 3.3)**	>10 (0)**	1.1 ± 0.10**
FTC	0.52 ± 0.12	3.0 ± 0.40**	>10 (0)**	0.22 ± 0.12
Adenosine analog				
TDF	0.0071 ± 0.0018	0.0016 ± 0.00025**	0.0071 ± 0.00056	0.0039 ± 0.0021
INSTI				
RAL	0.0033 ± 0.0010	0.0024 ± 0.00068	0.00064 ± 0.00057	0.062 ± 0.032**

^a Antiviral activities of NRTIs and an INSTI against VSV-G-pseudotyped SRV-4, HIV-1, MoMLV, and FIV were determined by using a luciferase assay. Data are shown as means and standard deviations obtained from three or more independent experiments, and statistical analyses were performed (*, $P < 0.05$; **, $P < 0.01$; not indicated, $P \geq 0.05$ [determined by Dunnett's test against control HIV-1]). EC₅₀s shown as >10 indicate that more than 10 μM drugs is required to block viral infection by 50%. In this case, percent inhibition of viral infection at 10 μM is shown in parentheses and is considered 10 μM for statistical analysis.

RESULTS

Anti-SRV-4 activity of HIV NRTIs in single-round infection. To date, there is no convenient assay system for evaluating the anti-SRV-4 activity of compounds; therefore, we first established a simple and quantitative assay system by employing VSV-G-pseudotyped luciferase-expressing SRV-4 as a model virus. The anti-SRV-4 activity of the test compounds was evaluated by using TE671 and MT-2 cells. TE671 cells, which are derived from human rhabdomyosarcoma, have frequently been used for infection experiments with several retroviruses, including SRVs (23). MT-2 cells, which are derived from human T lymphocytes, are also susceptible to some viruses, including HIV (24) and hepatitis C virus (25), and are routinely used for analysis of antiviral activity of inhibitors (9). Inhibitory activity against HIV-1 and FIV (lentiviruses) and MoMLV (gammaretrovirus) was also evaluated.

Some HIV NRTIs reportedly possess anti-SRV-1 and anti-SRV-2 activities (16, 18); therefore, we first evaluated the anti-SRV-4 activity of seven NRTIs which have been approved for the treatment of HIV-1-infected patients. When TE671 cells were

used as targets, ddI, ddC, and 3TC exhibited weak anti-SRV-4 activities, with EC₅₀s within the micromolar range (EC₅₀, 2.7 to 4.4 μM), whereas d4T and FTC exhibited moderate anti-SRV-4 activities, with EC₅₀s within the submicromolar range (EC₅₀, 0.2 and 0.5 μM, respectively) (Table 1). Remarkably, AZT and TDF exhibited potent anti-SRV-4 activities, with EC₅₀s of 42 and 0.8 nM, respectively. In contrast, almost all the NRTIs showed higher EC₅₀s using MT-2 cells as targets than those using TE671 cells as targets (Table 1). However, AZT and TDF exerted potent anti-SRV-4 activities, with EC₅₀s of 110 and 1.6 nM, respectively, even in the less sensitive MT-2 cells. Notably, all the NRTIs tested in this study exhibited no cytotoxicity against both cell types up to 100 μM, indicating that the observed anti-SRV-4 activity was not because of cell damage (data not shown).

One possible explanation for the difference in drug susceptibility between TE671 and MT-2 cells would be the different phosphorylation efficacies of NRTIs, which require sequential phosphorylations by cellular kinases to reach the active form (26, 27). To confirm this, we next evaluated anti-HIV-1, anti-FIV, and an-

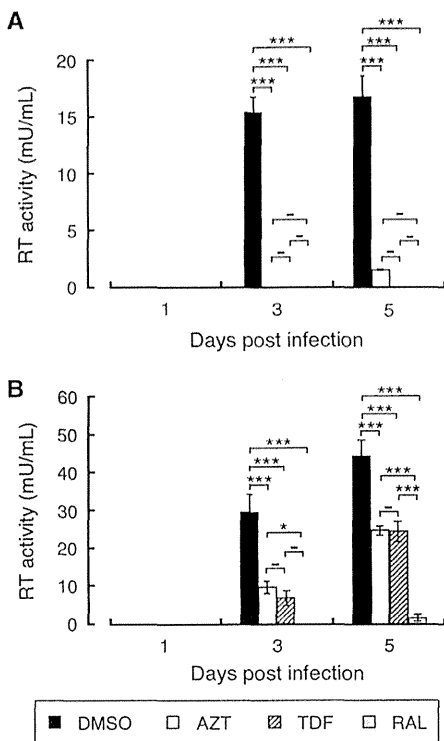


FIG 1 Effects of AZT, TDF, and RAL on SRV-4 replication. Anti-SRV-4 activities of AZT, TDF, and RAL were evaluated in cell-free transmission (A) and cell-to-cell transmission (B) models. SRV-4-free 293T cells were treated with AZT (400 nM), TDF (10 nM), RAL (150 nM), or vehicle (DMSO). After 4 h, culture media were replaced with fresh medium containing identical concentrations of each drug with replication-competent SRV-4 (A) or with SRV-4-infected 293T cells at a ratio of uninfected to infected cells of 50:1 (B). Culture supernatants were periodically collected, and SRV-4 was concentrated. The viral pellet was lysed, and reverse transcriptase activity derived from SRV-4 was quantified with a standard of known activity to monitor viral production. Data are shown as means and standard deviations obtained from three independent experiments. *, $P < 0.05$; **, $P < 0.01$; ***, $P < 0.001$; –, $P \geq 0.05$ (determined by the Bonferroni test).

ti-MoMLV activities using the same assay system, in which TE671 or MT-2 cells were infected with VSV-G-pseudotyped luciferase-expressing HIV-1- or FIV-based lentiviral vectors or MoMLV-based retroviral vectors in the presence of various concentrations of inhibitors. HIV-1 infection was blocked by all the tested NRTIs to various extents (Table 1). Among these, AZT and TDF exhibited potent activities against SRV-4 and MoMLV infections, while d4T was less active than AZT (Table 1). In FIV infection, AZT and d4T were active within the submicromolar range only in TE671 cells; however, TDF exhibited potent anti-FIV activity in both cell types (Table 1). Importantly, variation of EC_{50} s of NRTIs against HIV-1 was minimum between both target cell types (0.3- to 2.1-fold change in EC_{50} s measured with TE671 and MT-2 cells), suggesting that cell-derived factors are not a major cause of target cell-based differences in anti-SRV-4 activity.

Taken together, these findings indicate that HIV NRTIs have inhibitory activity against SRV-4 infection to various extents. Among these, AZT showed preferential anti-SRV-4 activity, a trend different from that previously observed against SRV-1 and SRV-2 (18). In addition, TDF exhibited the most potent anti-SRV-4 activity in the single-round infection assay.

Inhibitory effect of HIV-1 NNRTIs on SRV-4 infection.

HIV-1 NNRTIs, including NVP and EFV, efficiently suppress HIV-1 infection by inhibiting HIV-1 RT activity by binding to a hydrophobic pocket near the RT polymerase active site (28, 29). In the present study, EFV showed slight cytotoxicity, with CC_{50} values of 57 and 48 μ M in TE671 and MT-2 cells, respectively. However, both NVP and EFV potently inhibited HIV-1 infection, with EC_{50} s within the nanomolar to subnanomolar range (0.57 to 82 nM) in both cell types. In contrast, NVP and EFV were completely inactive against SRV-4 infection as well as against MoMLV and FIV infections, even at 10 μ M. These results correlate well with the impressive narrow spectrum of NNRTI activity; i.e., NNRTIs are active against HIV-1 but not against HIV-2 and other retroviruses (11, 30–32).

Inhibitory activity of an HIV INSTI against SRV-4 infection.

We next evaluated the inhibitory effect of RAL, the first INSTI approved for clinical use, on SRV-4 infection. RAL has potent anti-HIV-1 activity in addition to a broad antiviral spectrum including simian immunodeficiency virus (SIV) (33), MLV (34), XMRV (11), and SRV-3 (19). We also observed that RAL inhibited HIV-1 and MoMLV infections (Table 1). FIV was less susceptible to RAL than HIV-1 and MoMLV, although the RAL EC_{50} against FIV was at the nanomolar level. Most importantly, SRV-4 infection was potently inhibited by RAL within a nanomolar concentration (Table 1). We previously observed that EVG, a new INSTI contained within a recently approved anti-HIV drug, was active against not only HIV but also MoMLV and SIV (9), indicating that INSTIs are a preferential class of inhibitors for a wide range of retroviral infections. We report for the first time the potential blockage of SRV-4 infection by RAL without cytotoxicity.

Effect of HIV PIs on SRV-4 production. We then evaluated the inhibitory activity of PIs against SRV-4 replication. It is impossible to evaluate the anti-SRV-4 activity of PIs with the replication-deficient SRV-4 used to evaluate the inhibitory activities of NRTIs, NNRTIs, and an INSTI. To overcome this limitation, we evaluated persistently SRV-4-infected cells, in which the production of progeny infectious virions from SRV-4-infected 293T cells was monitored in the presence of various concentrations of PIs. Viruses released into culture supernatants were quantified by virion-derived RT activity.

First, we measured the cytotoxicity of three PIs (NFV, SQV, and DRV) against 293T cells. Although DRV showed no cytotoxicity up to 100 μ M, NFV and SQV decreased cell viability, with CC_{50} values of 22 and 28 μ M, respectively. To exclude a cell toxicity-based reduction in viral production, we used 0.1 and 1 μ M concentrations of PIs in this study, which are sufficiently high to exert anti-HIV-1 activity (11, 35, 36). However, none of the PIs inhibited late-phase SRV-4 replication steps even at 1 μ M (data not shown), indicating that SRV-4 is intrinsically less susceptible to PIs.

Effects of AZT, TDF, and RAL on SRV-4 replication. As observed in the early part of this study, two NRTIs (AZT and TDF) and one INSTI (RAL) efficiently inhibited replication-deficient SRV-4 infection in a single-cycle luciferase assay. To further elucidate the anti-SRV-4 property of these inhibitors, we assessed their effect on SRV-4 replication.

To precisely evaluate the inhibitory activity against SRV-4 replication, we distinguished the SRV-4 replication pattern into two viral expansion pathways: cell-free and cell-to-cell transmission. In the cell-free model, SRV-4-free 293T cells were infected with

cell-free SRV-4 in the presence of inhibitors, and further viral expansion was monitored by virus-derived RT activity. In contrast, SRV-4-infected 293T cells were used as the source of infection for cell-to-cell transmission.

We observed that in the cell-free model, SRV-4 efficiently infected 293T cells and reached the maximum level at 3 days postinfection (Fig. 1A). Similarly, viral expansion through *de novo* SRV-4 transmission was observed in the cell-to-cell model (Fig. 1B). However, SRV-4 expanded more efficiently through the cell-to-cell mechanism than through the cell-free mechanism, as judged by the 2- to 3-fold-higher RT activity observed in the cell-to-cell model at 5 days postinfection, indicating that cell-derived SRV-4 is a favorable source of SRV-4. Under these conditions, the 10-fold-higher EC_{50} s of AZT, TDF, and RAL, previously measured in single-round infection assays, completely inhibited cell-free SRV-4 infection up to 3 days (Fig. 1A). However, on day 5, only 7% of the viral production was observed in the presence of AZT, whereas TDF and RAL still almost completely blocked SRV-4 expansion. This tendency was well correlated with the antiviral activity measured during the single-round SRV-4 infection (Table 1). In contrast, when cell-associated SRV-4 was used as the infectious source, inhibitory activities of AZT and TDF were only partial; therefore, *de novo* SRV-4 transmission was ongoing at 3 and 5 days postinfection (Fig. 1B). Notably, we sequenced the RT regions of the proviral DNA at the end of this study, and no changes from the original SRV-4 were observed (data not shown). Thus, drug resistance was not associated with insufficient activity. However, only 3% to 5% of viral replication was observed in the presence of RAL on day 5 ($P < 0.001$, compared to AZT and TDF), indicating that RAL potentially inhibited SRV-4 replication; therefore, it should be highly effective in controlling SRV-4 infection and replication.

DISCUSSION

To date, several SRV serotypes have been identified, and their distributions in monkeys have been revealed (1–3, 37–41). For example, SRV-4 and SRV-5 infect cynomolgus and rhesus monkeys, respectively, while the Japanese monkey is not a natural host of these SRVs (7, 42). However, the recent outbreak of SRV-4 at PRI revealed that Japanese monkeys are susceptible to SRV-4 (5), since fatal disease could be induced in some of them (43) (Okamoto et al., unpublished). These epidemics reflect the necessity for effective drugs against SRV-4 infection. In addition, human SRV infection has been reported, although no associated diseases have been identified (44). This finding also suggests that the identification of anti-SRV drugs is important to prevent the entry of these viruses into the human population.

Among the identified SRVs, the inhibitory activity of anti-HIV drugs against SRV-1 and SRV-2 has been relatively well analyzed. In these studies, the evaluation of anti-SRV activity was performed by time-consuming, cost-intensive, and hazardous procedures, e.g., using wild-type SRVs and infected monkeys (17, 18). In the present study, we used a VSV-G-pseudotyped luciferase reporter SRV-4 to screen inhibitors with anti-SRV-4 activity from a panel of clinically approved anti-HIV drugs. In this system, the luciferase reporter gene enabled sensitive and rapid evaluation. Moreover, replacement of the intrinsic envelope with VSV-G avoids the restriction of target cell tropism, thereby enabling the direct comparison of antiviral activity with other viruses in the same cells. Using this assay system, we reported for the first time that two

anti-HIV NRTIs (AZT and TDF) and one INSTI (RAL) efficiently inhibited SRV-4 infection. The tendency for drug susceptibility of SRV-4 is different from that of SRV-1 and SRV-2, as reported in a previous study in which SRV-1 and SRV-2 infections were more potentially inhibited by ddC than by AZT, 3TC, and d4T (18). Reportedly, SRV-4 is genetically distinct from SRV-1 and SRV-2 (3), suggesting that this intrinsic diversity reflects drug susceptibility.

Among the NRTIs tested, AZT and TDF exhibited potent anti-SRV-4 activities in single-round infection and cell-free viral transmission and also inhibited HIV-1, MoMLV, and FIV infections to various extents. However, the inhibitory activities of some NRTIs, particularly the thymidine analogs AZT and d4T, against SRV-4, MoMLV, and FIV infections were markedly (>10-fold) varied between TE671 and MT-2 cells (Table 1). A similar variation was previously reported for several viruses (18, 45). Major factors accounting for the different sensitivities of viruses to NRTIs in different target cells include the endogenous levels of some kinases as well as the levels of the intracellular pool of nucleotides (45–47). Moreover, although HIV-1 preferentially infects lymphoid cells, SRV infects a wide variety of cells, including not only CD4⁺, CD8⁺, and B cells *in vivo* but also lung fibroblast and kidney cells of monkeys *in vitro* (48). It is likely that the nature of the virus and assay conditions affects the susceptibility of SRV-4 to NRTIs in different cells, although further analyses are required to completely elucidate this phenomenon. TDF preferentially inhibited all the tested retroviruses. All the nucleoside-type RT inhibitors required three sequential phosphorylations, whereas TDF requires only a two-step phosphorylation to be active (49, 50), suggesting that this kinetic advantage reflects potent antiviral properties.

To gain deeper insights into the drug susceptibility of SRV-4, amino acid sequences of regions corresponding to the RT-polymerase domain (residues 63 to 234 of HIV-1) and the integrase catalytic core domain (IN-CCD) (residues 50 to 212) were compared with those of HIV-1, MoMLV, and FIV (Fig. 2). Because genotypic studies to elucidate drug susceptibility based on amino acid changes have been extensively performed for HIV-1 (22, 51, 52), we applied those observations to genotypic analysis of SRV-4. Overall, we confirmed that some amino acid residues in SRV-4 are identical to reported mutations affecting drug susceptibility in HIV-1. For example, HIV-1 RT mutations at positions 41, 67, 70, 210, 215, and 219, known as thymidine analog mutations (TAMs), are frequently observed in AZT and D4T resistance (52–54). In SRV-4 RT, some residues corresponding to TAMs differ from those of wild-type HIV-1 (Fig. 2A), although they must not be involved in drug susceptibility of SRV-4, since AZT and d4T inhibited SRV-4 infection at a similar or superior level compared to HIV-1 infection. In addition, although mutations at Q151 in the LPQG motif and M184 in the YMDD motif are involved in higher-level resistance to some NRTIs (55–57), these motifs are completely conserved in SRV-4 RT. In contrast, MoMLV showed complete insensitivity to certain NRTIs, including 3TC, at 10 μ M (Table 1), in agreement with previous reports (8, 18). Taken together, as apparent from genotypic analysis of SRV-4 RT, AZT and TDF are thought to be potent therapeutic agents for the inhibition and control of SRV-4.

RAL, an HIV INSTI, showed potent inhibitory activity against SRV-4 infection as well as against HIV-1, MoMLV, and FIV infections. HIV-1 acquires high-level RAL resistance by mutations such as Q148H/R/K and N155H (52, 58). Although SRV-4 IN

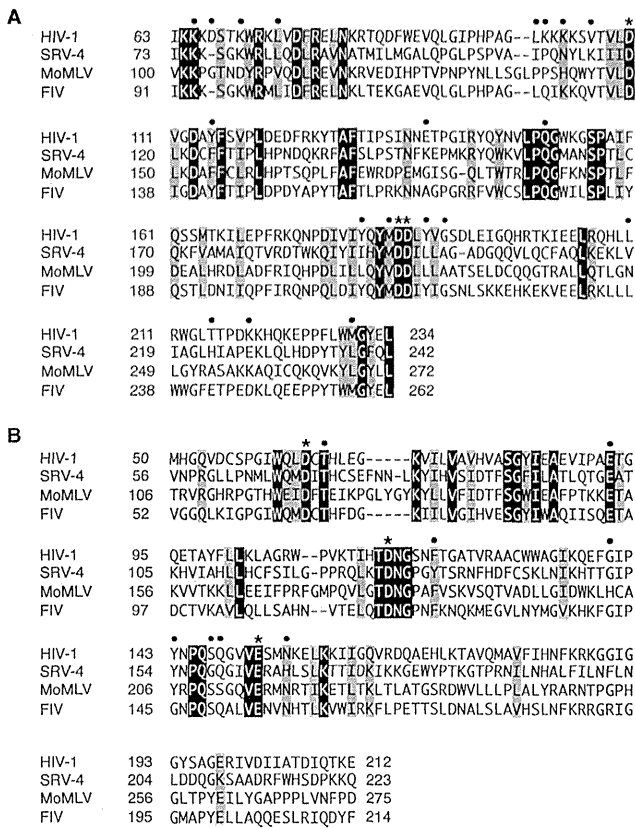


FIG 2 Protein sequence alignments of RT and IN. Reference amino acid sequences of SRV-4 (GenBank accession number NC_014474.1), HIV-1 (accession number NC_001802.1), MoMLV (accession number NC_001501.1), and FIV (accession number NC_001482.1) were aligned by using the program Clustal W, and the regions corresponding to the RT-polymerase domain (residues 63 to 234) (A) and the IN catalytic core domain (residues 50 to 212) (B) of HIV-1 are shown. The amino acid numbering of SRV-4 IN is based on that of SRV-3 (68). Absolutely conserved residues and conserved substitutions are shown in black and gray boxes, respectively. For symbols above the sequences, closed circles indicate residues associated with drug resistance for HIV-1, and asterisks indicate catalytic residues.

contains H166, which corresponds to N155 in HIV-1 (Fig. 2B), SRV-4 retained susceptibility within levels similar to those of wild-type HIV-1 (Table 1). Reportedly, SRV-3 also contains amino acids corresponding to N155H and F121Y, which are other INSTI resistance mutations; however, SRV-3 shows complete susceptibility to RAL (19). In contrast, bovine immunodeficiency virus (BIV) reportedly showed 23-fold resistance to RAL compared to wild-type HIV-1, although BIV contains a histidine (H) residue at the position corresponding to N155 (19), as seen in SRV-4, indicating that N155H is not a determinant of RAL susceptibility in retroviruses other than HIV. Although in the present study, FIV showed less susceptibility to RAL than the other retroviruses/lentiviruses tested (Table 1), FIV does not contain major INSTI resistance mutations. However, one distinct difference was observed: FIV IN carries G145, whereas it corresponds to Y143 in HIV-1 (Fig. 2B). The Y143G mutation has rarely been observed in RAL-treated patients (59); therefore, the precise effect of this mutation on RAL resistance remains unclear. However, it was speculated that the Y143G mutation lacks the interaction with

RAL (19), and interestingly, Y143G reportedly affects proviral formation (60), although this is apparent in nondividing cells (61), likely suggesting that FIV IN G145 affects susceptibility of FIV not only to INSTIs but also to NRTIs.

To expand viral infection *in vitro* and *in vivo*, viruses utilize two main pathways: cell-free and cell-to-cell transmission. However, the transmission pathway depends on the nature of the viruses. For example, cell-free HIV-1 efficiently infects CD4⁺ T cells and also spreads in a cell-to-cell manner, whereas HTLV-1 transmits exclusively by a cell-to-cell pathway (62–66). In the present study, we compared the inhibitory activities of some inhibitors against SRV-4 replication in both cell-free and cell-to-cell transmission. We observed that although AZT and TDF could almost completely block cell-free SRV-4 transmission, they showed only marginal effects on cell-to-cell SRV-4 transmission (Fig. 1). In contrast, RAL completely suppressed SRV-4 replication in both cell-free and cell-to-cell transmission. These results indicate that a favorable pathway is intrinsically present in anti-HIV-1 drugs; AZT and TDF preferentially block cell-free infection, whereas RAL is active in both the pathways. A similar observation was reported for HIV-1, in which tenofovir preferentially suppressed cell-free transmission compared with cell-to-cell transmission (67). These observations may highlight the importance of the kinetics of viral replication and drug activation because AZT and TDF require tri- and diphosphorylation, respectively, to become active metabolites, whereas RAL does not require any modification to exert its antiviral activity. In addition, it is likely that the kinetics of SRV-4 replication steps, including reverse transcription and integration, vary between cell-free and cell-to-cell transmission, as seen for HIV-1; this may be another determinant of viral transmission pathway-dependent anti-SRV-4 activities.

Taken together, the present study demonstrated that AZT, TDF, and RAL potently inhibited SRV-4 infection. These inhibitors suppressed single-round infection and cell-free virus transmission of SRV-4; however, cell-to-cell transmission was blocked only by RAL. To effectively control SRV-4 infection and maintain a minimum risk of the emergence of drug resistance, a combination therapy of drugs such as ART in HIV-1 infection is important.

ACKNOWLEDGMENTS

We thank H. Miyoshi and Y. Sakurai for providing lentiviral vectors and the pDON-AI-2-luc vector, respectively. The following reagents were obtained through the NIH AIDS Research and Reference Reagent Program, Division of AIDS, NIAID, NIH: emtricitabine, tenofovir disoproxil fumarate, darunavir (from Tibotec, Inc.), and raltegravir (from Merck & Company, Inc.).

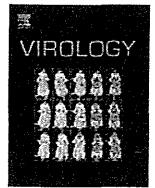
This work was supported in part by a JSPS KAKENHI grant-in-aid for young scientists (B) to K.S. (grant number 24791021) and a grant-in-aid for scientific research (B) to M.O. (grant number 24300153).

REFERENCES

- Daniel MD, King NW, Letvin NL, Hunt RD, Sehgal PK, Desrosiers RC. 1984. A new type D retrovirus isolated from macaques with an immunodeficiency syndrome. *Science* 223:602–605.
- Marx PA, Maul DH, Osborn KG, Lerche NW, Moody P, Lowenstine LJ, Henrickson RV, Arthur LO, Gildea RV, Gravell M. 1984. Simian AIDS: isolation of a type D retrovirus and transmission of the disease. *Science* 223:1083–1086.
- Montiel NA. 2010. An updated review of simian betaretrovirus (SRV) in macaque hosts. *J. Med. Primatol.* 39:303–314.
- Henrickson RV, Maul DH, Lerche NW, Osborn KG, Lowenstine LJ, Prahalada S, Sever JL, Madden DL, Gardner MB. 1984. Clinical features

- of simian acquired immunodeficiency syndrome (SAIDS) in rhesus monkeys. *Lab. Anim. Sci.* 34:140–145.
5. CDC-KUPRI. 2010. Information of hemorrhagic syndrome of Japanese macaques (provisional designation). *Primate Res.* 26:69–71.
 6. Zao CL, Armstrong K, Tomanek L, Cooke A, Berger R, Estep JS, Marx PA, Trask JS, Smith DG, Yee JL, Lerche NW. 2010. The complete genome and genetic characteristics of SRV-4 isolated from cynomolgus monkeys (*Macaca fascicularis*). *Virology* 405:390–396.
 7. Zao CL, Ward JA, Tomanek L, Cooke A, Berger R, Armstrong K. 2011. Virological and serological characterization of SRV-4 infection in cynomolgus macaques. *Arch. Virol.* 156:2053–2056.
 8. Powell SK, Artlip M, Kaloss M, Brazinski S, Lyons R, McGarrity GJ, Otto E. 1999. Efficacy of antiretroviral agents against murine replication-competent retrovirus infection in human cells. *J. Virol.* 73:8813–8816.
 9. Shimura K, Kodama E, Sakagami Y, Matsuzaki Y, Watanabe W, Yamataka K, Watanabe Y, Ohata Y, Doi S, Sato M, Kano M, Ikeda S, Matsuoka M. 2008. Broad antiretroviral activity and resistance profile of the novel human immunodeficiency virus integrase inhibitor elvitegravir (JTK-303/GS-9137). *J. Virol.* 82:764–774.
 10. Sakuma R, Sakuma T, Ohmine S, Silverman RH, Ikeda Y. 2010. Xenotropic murine leukemia virus-related virus is susceptible to AZT. *Virology* 397:1–6.
 11. Smith RA, Gottlieb GS, Miller AD. 2010. Susceptibility of the human retrovirus XMRV to antiretroviral inhibitors. *Retrovirology* 7:70. doi:10.1186/1742-4690-7-70.
 12. Zhu YQ, Remington KM, North TW. 1996. Mutants of feline immunodeficiency virus resistant to 2',3'-dideoxy-2',3'-didehydrothymidine. *Antimicrob. Agents Chemother.* 40:1983–1987.
 13. North TW, North GL, Pedersen NC. 1989. Feline immunodeficiency virus, a model for reverse transcriptase-targeted chemotherapy for acquired immune deficiency syndrome. *Antimicrob. Agents Chemother.* 33:915–919.
 14. Matsushita S, Mitsuya H, Reitz MS, Broder S. 1987. Pharmacological inhibition of *in vitro* infectivity of human T lymphotropic virus type I. *J. Clin. Invest.* 80:394–400.
 15. Miyazato P, Yasunaga J, Taniguchi Y, Koyanagi Y, Mitsuya H, Matsuoka M. 2006. De novo human T-cell leukemia virus type 1 infection of human lymphocytes in NOD-SCID, common gamma-chain knockout mice. *J. Virol.* 80:10683–10691.
 16. Tsai CC, Follis KE, Benveniste RE. 1988. Antiviral effects of 3'-azido-3'-deoxythymidine, 2',3'-dideoxycytidine, and 2',3'-dideoxyadenosine against simian acquired immunodeficiency syndrome-associated type D retrovirus *in vitro*. *AIDS Res. Hum. Retroviruses* 4:359–368.
 17. Tsai CC, Follis KE, Yarnall M, Blakley GA. 1989. Toxicity and efficacy of 2',3'-dideoxycytidine in clinical trials of pigtailed macaques infected with simian retrovirus type 2. *Antimicrob. Agents Chemother.* 33:1908–1914.
 18. Rosenblum LL, Patton G, Grigg AR, Frater AJ, Cain D, Erlwein O, Hill CL, Clarke JR, McClure MO. 2001. Differential susceptibility of retroviruses to nucleoside analogues. *Antivir. Chem. Chemother.* 12:91–97.
 19. Koh Y, Matreyek KA, Engelman A. 2011. Differential sensitivities of retroviruses to integrase strand transfer inhibitors. *J. Virol.* 85:3677–3682.
 20. White JA, Todd PA, Rosenthal AN, Yee JL, Grant R, Lerche NW. 2009. Development of a generic real-time PCR assay for simultaneous detection of proviral DNA of simian betaretrovirus serotypes 1, 2, 3, 4 and 5 and secondary uniplex assays for specific serotype identification. *J. Virol. Methods* 162:148–154.
 21. Thompson JD, Higgins DG, Gibson TJ. 1994. CLUSTAL W: improving the sensitivity of progressive multiple sequence alignment through sequence weighting, position-specific gap penalties and weight matrix choice. *Nucleic Acids Res.* 22:4673–4680.
 22. Rhee SY, Gonzales MJ, Kantor R, Betts BJ, Ravela J, Shafer RW. 2003. Human immunodeficiency virus reverse transcriptase and protease sequence database. *Nucleic Acids Res.* 31:298–303.
 23. Tailor CS, Nouri A, Zhao Y, Takeuchi Y, Kabat D. 1999. A sodium-dependent neutral-amino-acid transporter mediates infections of feline and baboon endogenous retroviruses and simian type D retroviruses. *J. Virol.* 73:4470–4474.
 24. Harada S, Koyanagi Y, Yamamoto N. 1985. Infection of HTLV-III/LAV in HTLV-I-carrying cells MT-2 and MT-4 and application in a plaque assay. *Science* 229:563–566.
 25. Kato N, Nakazawa T, Mizutani T, Shimotohno K. 1995. Susceptibility of human T-lymphotropic virus type 1 infected cell line MT-2 to hepatitis C virus infection. *Biochem. Biophys. Res. Commun.* 206:863–869.
 26. Cihlar T, Ray AS. 2010. Nucleoside and nucleotide HIV reverse transcriptase inhibitors: 25 years after zidovudine. *Antiviral Res.* 85:39–58.
 27. Pillero PJ. 2004. Pharmacokinetic properties of nucleoside/nucleotide reverse transcriptase inhibitors. *J. Acquir. Immune Defic. Syndr.* 37(Suppl 1):S2–S12. <http://download.bion.com.cn/upload/201101/17/101159hswyecdh77cw6xv.attach.pdf>.
 28. Ren J, Stammers DK. 2008. Structural basis for drug resistance mechanisms for non-nucleoside inhibitors of HIV reverse transcriptase. *Virus Res.* 134:157–170.
 29. Huang H, Chopra R, Verdine GL, Harrison SC. 1998. Structure of a covalently trapped catalytic complex of HIV-1 reverse transcriptase: implications for drug resistance. *Science* 282:1669–1675.
 30. Auwerx J, Esnouf R, De Clercq E, Balzarini J. 2004. Susceptibility of feline immunodeficiency virus/human immunodeficiency virus type 1 reverse transcriptase chimeras to non-nucleoside RT inhibitors. *Mol. Pharmacol.* 65:244–251.
 31. Ren J, Bird LE, Chamberlain PP, Stewart-Jones GB, Stuart DI, Stammers DK. 2002. Structure of HIV-2 reverse transcriptase at 2.35-Å resolution and the mechanism of resistance to non-nucleoside inhibitors. *Proc. Natl. Acad. Sci. U. S. A.* 99:14410–14415.
 32. Witvrouw M, Pannecouque C, Switzer WM, Folks TM, De Clercq E, Heneine W. 2004. Susceptibility of HIV-2, SIV and SHIV to various anti-HIV-1 compounds: implications for treatment and postexposure prophylaxis. *Antivir. Ther.* 9:57–65.
 33. Lewis MG, Norelli S, Collins M, Barreca ML, Iraci N, Chirullo B, Yalley-Ogunro J, Greenhouse J, Titti F, Garaci E, Savarino A. 2010. Response of a simian immunodeficiency virus (SIVmac251) to raltegravir: a basis for a new treatment for simian AIDS and an animal model for studying lentiviral persistence during antiretroviral therapy. *Retrovirology* 7:21. doi:10.1186/1742-4690-7-21.
 34. Beck-Engeser GB, Eilat D, Harrer T, Jäck HM, Wabl M. 2009. Early onset of autoimmune disease by the retroviral integrase inhibitor raltegravir. *Proc. Natl. Acad. Sci. U. S. A.* 106:20865–20870.
 35. Koh Y, Nakata H, Maeda K, Ogata H, Bilcer G, Devasamudram T, Kincaid JF, Boross P, Wang YF, Tie Y, Volarath P, Gaddis L, Harrison RW, Weber IT, Ghosh AK, Mitsuya H. 2003. Novel bis-tetrahydrofuranylurethane-containing nonpeptidic protease inhibitor (PI) UIC-94017 (TMC114) with potent activity against multi-PI-resistant human immunodeficiency virus *in vitro*. *Antimicrob. Agents Chemother.* 47:3123–3129.
 36. Patick AK, Mo H, Markowitz M, Appelt K, Wu B, Musick L, Kalish V, Kaldor S, Reich S, Ho D, Webber S. 1996. Antiviral and resistance studies of AG1343, an orally bioavailable inhibitor of human immunodeficiency virus protease. *Antimicrob. Agents Chemother.* 40:292–297.
 37. Hara M, Sata T, Kikuchi T, Nakajima N, Uda A, Fujimoto K, Baba T, Mukai R. 2005. Isolation and characterization of a new simian retrovirus type D subtype from monkeys at the Tsukuba Primate Center, Japan. *Microbes Infect.* 7:126–131.
 38. Marx PA, Bryant ML, Osborn KG, Maul DH, Lerche NW, Lowenstine LJ, Kluge JD, Zaiss CP, Henrickson RV, Shiigi SM. 1985. Isolation of a new serotype of simian acquired immune deficiency syndrome type D retrovirus from Celebes black macaques (*Macaca nigra*) with immune deficiency and retroperitoneal fibromatosis. *J. Virol.* 56:571–578.
 39. Nandi JS, Bhavalkar-Potdar V, Tikute S, Raut CG. 2000. A novel type D simian retrovirus naturally infecting the Indian Hanuman langur (*Semnopithecus entellus*). *Virology* 277:6–13.
 40. Nandi JS, Tikute SA, Chhangani AK, Potdar VA, Tiwari-Mishra M, Ashtekar RA, Kumari J, Walimbe A, Mohnot SM. 2003. Natural infection by simian retrovirus-6 (SRV-6) in Hanuman langurs (*Semnopithecus entellus*) from two different geographical regions of India. *Virology* 311:192–201.
 41. Nandi JS, Van Dooren S, Chhangani AK, Mohnot SM. 2006. New simian beta retroviruses from rhesus monkeys (*Macaca mulatta*) and langurs (*Semnopithecus entellus*) from Rajasthan, India. *Virus Genes* 33:107–116.
 42. Li B, Axthelm MK, Machida CA. 2000. Simian retrovirus serogroup 5: partial gag-prt sequence and viral RNA distribution in an infected rhesus macaque. *Virus Genes* 21:241–248.
 43. Cyranoski D. 2010. Japanese monkey deaths puzzle. *Nature* 466:302–303.
 44. Lerche NW, Switzer WM, Yee JL, Shanmugam V, Rosenthal AN, Chapman LE, Folks TM, Heneine W. 2001. Evidence of infection with simian type D retrovirus in persons occupationally exposed to nonhuman primates. *J. Virol.* 75:1783–1789.

45. Dahlberg JE, Mitsuya H, Blam SB, Broder S, Aaronson SA. 1987. Broad spectrum antiretroviral activity of 2',3'-dideoxynucleosides. *Proc. Natl. Acad. Sci. U. S. A.* 84:2469–2473.
46. Balzarini J. 2000. Effect of antimetabolite drugs of nucleotide metabolism on the anti-human immunodeficiency virus activity of nucleoside reverse transcriptase inhibitors. *Pharmacol. Ther.* 87:175–187.
47. Ray AS. 2005. Intracellular interactions between nucleos(t)ide inhibitors of HIV reverse transcriptase. *AIDS Rev.* 7:113–125.
48. Maul DH, Zaiss CP, MacKenzie MR, Shiigi SM, Marx PA, Gardner MB. 1988. Simian retrovirus D serogroup 1 has a broad cellular tropism for lymphoid and nonlymphoid cells. *J. Virol.* 62:1768–1773.
49. De Clercq E, Holý A. 2005. Acyclic nucleoside phosphonates: a key class of antiviral drugs. *Nat. Rev. Drug Discov.* 4:928–940.
50. De Clercq E. 2009. The history of antiretrovirals: key discoveries over the past 25 years. *Rev. Med. Virol.* 19:287–299.
51. Shafer RW. 2006. Rationale and uses of a public HIV drug-resistance database. *J. Infect. Dis.* 194(Suppl 1):S51–S58. doi:10.1086/505356.
52. Johnson VA, Calvez V, Günthard HF, Paredes R, Pillay D, Shafer R, Wensing AM, Richman DD. 2011. 2011 update of the drug resistance mutations in HIV-1. *Top. Antivir. Med.* 19:156–164.
53. Gao Q, Gu ZX, Parniak MA, Li XG, Wainberg MA. 1992. In vitro selection of variants of human immunodeficiency virus type 1 resistant to 3'-azido-3'-deoxythymidine and 2',3'-dideoxyinosine. *J. Virol.* 66:12–19.
54. Lin PF, Samanta H, Rose RE, Patick AK, Trimble J, Bechtold CM, Revie DR, Khan NC, Federici ME, Li H. 1994. Genotypic and phenotypic analysis of human immunodeficiency virus type 1 isolates from patients on prolonged stavudine therapy. *J. Infect. Dis.* 170:1157–1164.
55. Quan Y, Gu Z, Li X, Liang C, Parniak MA, Wainberg MA. 1998. Endogenous reverse transcriptase assays reveal synergy between combinations of the M184V and other drug resistance-conferring mutations in interactions with nucleoside analog triphosphates. *J. Mol. Biol.* 277:237–247.
56. Shirasaka T, Kavlick MF, Ueno T, Gao WY, Kojima E, Alcaide ML, Choekijchai S, Roy BM, Arnold E, Yarchoan R. 1995. Emergence of human immunodeficiency virus type 1 variants with resistance to multiple dideoxynucleosides in patients receiving therapy with dideoxynucleosides. *Proc. Natl. Acad. Sci. U. S. A.* 92:2398–2402.
57. Tisdale M, Kemp SD, Parry NR, Larder BA. 1993. Rapid in vitro selection of human immunodeficiency virus type 1 resistant to 3'-thiacytidine inhibitors due to a mutation in the YMDD region of reverse transcriptase. *Proc. Natl. Acad. Sci. U. S. A.* 90:5653–5656.
58. Fransen S, Gupta S, Danovich R, Hazuda D, Miller M, Witmer M, Petropoulos CJ, Huang W. 2009. Loss of raltegravir susceptibility by human immunodeficiency virus type 1 is conferred via multiple nonoverlapping genetic pathways. *J. Virol.* 83:11440–11446.
59. Canducci F, Sampaolo M, Marinozzi MC, Boeri E, Spagnuolo V, Galli A, Castagna A, Lazzarin A, Clementi M, Gianotti N. 2009. Dynamic patterns of human immunodeficiency virus type 1 integrase gene evolution in patients failing raltegravir-based salvage therapies. *AIDS* 23:455–460.
60. Ikeda T, Nishitsuji H, Zhou X, Nara N, Ohashi T, Kannagi M, Masuda T. 2004. Evaluation of the functional involvement of human immunodeficiency virus type 1 integrase in nuclear import of viral cDNA during acute infection. *J. Virol.* 78:11563–11573.
61. Tsurutani N, Kubo M, Maeda Y, Ohashi T, Yamamoto N, Kannagi M, Masuda T. 2000. Identification of critical amino acid residues in human immunodeficiency virus type 1 IN required for efficient proviral DNA formation at steps prior to integration in dividing and nondividing cells. *J. Virol.* 74:4795–4806.
62. Igakura T, Stinchcombe JC, Goon PK, Taylor GP, Weber JN, Griffiths GM, Tanaka Y, Osame M, Bangham CR. 2003. Spread of HTLV-1 between lymphocytes by virus-induced polarization of the cytoskeleton. *Science* 299:1713–1716.
63. Jolly C, Kashafi K, Hollinshead M, Sattentau QJ. 2004. HIV-1 cell to cell transfer across an Env-induced, actin-dependent synapse. *J. Exp. Med.* 199:283–293.
64. Sattentau Q. 2008. Avoiding the void: cell-to-cell spread of human viruses. *Nat. Rev. Microbiol.* 6:815–826.
65. Pais-Correia AM, Sachse M, Guadagnini S, Robbiati V, Lasserre R, Gessain A, Gout O, Alcover A, Thoulouze MI. 2010. Biofilm-like extracellular viral assemblies mediate HTLV-1 cell-to-cell transmission at virological synapses. *Nat. Med.* 16:83–89.
66. Matsuoka M, Jeang KT. 2007. Human T-cell leukaemia virus type 1 (HTLV-1) infectivity and cellular transformation. *Nat. Rev. Cancer* 7:270–280.
67. Sigal A, Kim JT, Balazs AB, Dekel E, Mayo A, Milo R, Baltimore D. 2011. Cell-to-cell spread of HIV permits ongoing replication despite antiretroviral therapy. *Nature* 477:95–98.
68. Šnásel J, Krejčík Z, Jencová V, Rosenberg I, Ruml T, Alexandratos J, Gustchina A, Pichová I. 2005. Integrase of Mason-Pfizer monkey virus. *FEBS J.* 272:203–216.



Complementary and synergistic activities of anti-V3, CD4bs and CD4i antibodies derived from a single individual can cover a wide range of HIV-1 strains



Kristel Paola Ramirez Valdez^a, Takeo Kuwata^a, Yasuhiro Maruta^a, Kazuki Tanaka^a, Muntasir Alam^a, Kazuhisa Yoshimura^{a,b}, Shuzo Matsushita^{a,*}

^a Matsushita Project Laboratory, Center for AIDS Research, Kumamoto University, Kumamoto, Japan

^b AIDS Research Center, National Institute of Infectious Diseases, Tokyo, Japan

ARTICLE INFO

Article history:

Received 24 September 2014

Returned to author for revisions

17 October 2014

Accepted 10 November 2014

Available online 5 December 2014

Keywords:

HIV-1

Conventional antibodies

Neutralizing antibodies

Synergy

ADCC activity

ABSTRACT

Antibodies with modest neutralizing activity and narrow breadth are commonly elicited in HIV-1. Here, we evaluated the complementary and synergistic activities of a set of monoclonal antibodies (MAB) isolated from a single patient, directed to V3, CD4 binding site (CD4bs), and CD4 induced (CD4i) epitopes. Despite low somatic hypermutation percentages in the variable regions, these MABs covered viral strains from subtypes B, C, A and CRF01_AE and transmitted/founder viruses in terms of binding, neutralizing and antibody-dependent cell-mediated cytotoxicity (ADCC) activities. In addition, a combination of the anti-V3 and CD4bs MABs showed a synergistic effect over the neutralization of HIV-1_{JR-FL}. A humoral response from a single patient covered a wide range of viruses by complementary and synergistic activities of antibodies with different specificities. Inducing a set of narrow neutralizing antibodies, easier to induce than the broadly neutralizing antibodies, could be a strategy for developing an effective vaccine against HIV-1.

© 2014 Elsevier Inc. All rights reserved.

Introduction

Despite the great advances in the treatment of HIV-1 infection, there are still major obstacles to effective control of HIV-1 infection. Active replication persistence and immune activation under suppressive highly active antiretroviral therapy (HAART) (Buzon et al., 2010; Palmer et al., 2008; Richman et al., 2009), secondary effects of the drugs (Montessori et al., 2004; Reust, 2011), and the socio-economic burden of long-term treatment (Boyer, 2009; Naik et al., 2009) are still present; making the development of a protective vaccine desirable. Neutralizing antibodies are an important component of a protective vaccine-induced immune responses and much effort has been focused on the development of broadly neutralizing antibodies against conserved epitopes on the functional Env trimer of HIV-1 (Bonsignori et al., 2011; Corti et al., 2010; Walker et al., 2009).

Advances in antibody technology have uncovered broadly neutralizing Abs (bNAbs) (Marasco and Sui, 2007; Zhu et al., 2013; Zuo et al., 2011) and their efficacy has been proved in non-human animal models. Protection from infection by Simian immunodeficiency virus

(SIV) was correlated with the humoral response produced after vaccination with Env and/or Gag and Pol of rhesus macaques (Barouch et al., 2013; Roederer et al., 2014). Protection was also observed in rhesus macaques vaccinated with Env derived peptides and challenged with chimeric simian-human immunodeficiency viruses (SHIV) SHIV_{162P3} and SHIV_{C2/1} (DeVico et al., 2007; Eda et al., 2006a). Passive administration of antibodies was also proved useful in protecting for and controlling SHIV and HIV-1 infection. In rhesus macaques chronically infected with SHIV_{162P3}, passive administration of bNAbs (PGT121, 3BNC117 and b12 combined or alone) reduced viral load and resulted in control of the infection (Barouch et al., 2013; Ng et al., 2010). Similar results were observed in humanized mice chronically infected with HIV-1_{YU2} after the passive administration of bNAbs 45–46^{G54W}, PG16, PGT128, 10-1074 and 3BC176 (Klein et al., 2012). Passive administration of MABs PGT121, b12, 2G12, 2F5 and 4E10 also offered protection from infection with SHIV (Hessell et al., 2010, 2009a, 2009b; Mascola et al., 2000, 1999; Moldt et al., 2012; Parren et al., 2001) even when the antibody (b12) was administered topically (Veazey et al., 2003); or when the administered antibodies were purified IgG from infected chimpanzees (Shibata et al., 1999).

It has been proposed that an immunization strategy that could elicit such antibodies would be protective in humans (Stamatatos

* Corresponding author. Fax: +81 96 373 6537.

E-mail address: shuzo@kumamoto-u.ac.jp (S. Matsushita).

et al., 2009); however, to date there is no vaccine that induces their production.

In naturally infected HIV-1 patients, bNAbs are not commonly produced; instead, antibodies are often directed against strain-specific or non-neutralizing sites in Env (Burton et al., 1991; Corti et al., 2010). Only 10 to 25% of HIV-1-infected individuals generate neutralizing antibodies, and a minority of these individuals, approximately around 1%, is considered elite neutralizers, besides, bNAbs appear late (1 to 3 years) after infection (Binley et al., 2008; Deeks et al., 2006; Dhillon et al., 2007; Doria-Rose et al., 2010, 2009; Gray et al., 2011; Sather et al., 2009; Simek et al., 2009) and frequently harbor uncommon characteristics which probably pose obstacles to their generation, including high levels of somatic mutations, long heavy-chain complementarity-determining regions 3 (CDRH3s), frequent insertions or deletions, and high levels of polyreactivity (Haynes et al., 2012b; Huber et al., 2010; Klein et al., 2013; Scheid et al., 2011; Sok et al., 2013; Xiao et al., 2009). Moreover, when the immunoglobulin sequences of bNAbs are experimentally reverted to their germline precursors, as they are found on naive B cells, binding to HIV-1 Env is often significantly diminished or even completely abrogated (Bonsignori et al., 2011; Haynes et al., 2012b; McGuire et al., 2014; Scheid et al., 2011; Wu et al., 2011; Xiao et al., 2009). This suggests difficulties in inducing bNAbs in HIV-1-infected patients and also by vaccination, because many rounds of affinity maturation are required which means that immunizations should be repeated many times as well.

Antibodies to the V3 loop, CD4bs and CD4i have been produced by HIV infection or vaccination, but neutralization by these antibodies is generally not broadly effective for preventing HIV-1 infection because of steric constraints blocking the access of these antibodies to the epitopes, and mutations in their epitopes that allow to escape from these antibodies. However, these modest neutralizing antibodies appear faster after infection (even as early as 2 weeks after sero-conversion) and are also capable of exert pressure over the virus (Bar et al., 2012; Haynes et al., 2012b; McGuire et al., 2014; Overbaugh and Morris, 2012; Pollara et al., 2014).

Besides neutralization, non-neutralizing responses, specifically the ADCC activity has been associated with protection from HIV. The most remarkable case is the RV144 trial result, which showed a 31.2% of vaccine efficacy (Rerks-Ngarm et al., 2009) and it has been proposed that the ADCC activity of V1/V2 antibodies induced by the vaccine may be the most important correlation for protection (Haynes et al., 2012a; Rerks-Ngarm et al., 2009; Wren et al., 2012). Vaccination in animal models has shown similar results (Hessell et al., 2007; Xiao et al., 2010) and it has also been reported that broader ADCC responses correlate with long-term control of HIV, slow progression of disease and lower viremia (Nag et al., 2004; Wren et al., 2013; Xiao et al., 2010).

It is certainly desirable for HIV-vaccines to induce antibodies that neutralize global isolates of diverse subtypes. However, in view of the difficulty in inducing bNAbs in uninfected subjects, the induction of a complementary set of antibodies with limited neutralizing activity may be an attainable alternative approach. We have been following a single patient infected with HIV that has a cross-neutralizing activity to a variety of HIV-1 isolates including a panel of clinical isolates belonging to subtypes B, C, CRF01_AE and A. The patient is a hemophiliac who has been infected with HIV-1 for more than 25 years without any antiretroviral treatment. To elucidate the mechanism to control viruses in this patient we established a series of MAbs and demonstrated that a combination of antibodies to the V3 loop, CD4bs and CD4i covered effectively a wide range of viruses by their complementary and synergistic activities.

Results

Isolation and classification of monoclonal antibodies from an HIV-1 infected patient with long-term non-progressive disease

A total of 1718 B-cell clones were established by Epstein-Barr virus (EBV) transformation from the patient KTS376 who has had controlled HIV-1 infection for more than 25 years without any

Table 1
Subclass, target and genetic characteristics of human monoclonal antibodies against HIV-1 obtained from a patient with non-progressive disease.

No	Clone	Subclass	Target	Gene usage		Somatic mutation (%)		CDRH3 length
				VH	VL	VH	VL	
1	0.5γ (1C10)	IgG1κ	V3	VH3-30	VK2-28	10.8	4.1	18
2	1D9	IgG1κ	V3	VH3-30	VK2-28	12.8	3.5	16
3	5G2	IgG1κ	V3	VH3-30	VK2-28	12.8	6.5	16
4	16G6	IgG1λ	V3	VH5-51	VL3-19	4.9	6.4	7
5	717G2	IgG2κ	V3	VH3-30	VK2D-29	10.8	7.1	21
6	2F8	IgG1λ	V3	-	-	-	-	-
7	3E4	IgG1κ	V3	-	-	-	-	-
8	3G8	IgG1κ	V3	-	-	-	-	-
9	42F9	IgG1κ	CD4bs	VH3-20	VK1-39	2	2.5	19
10	49G2	IgG1λ	CD4bs	VH1-18	VL1-44	5.9	1.8	22
11	82D5	IgG1λ	CD4bs	VH1-18	VL1-44	6.2	1.7	22
12	0.5δ(3D6)	IgG1λ	CD4bs	-	-	-	-	-
13	4E3	IgG1κ	CD4bs	-	-	-	-	-
14	7B5	IgG2λ	CD4bs	-	-	-	-	-
15	4E9C	IgG1κ	CD4i	VH1-69	VK3-15	6.6	1.8	22
16	916B2	IgG1λ	CD4i	VH1-69	VL7-46	8.7	5.9	16
17	917B11	IgG1λ	CD4i	VH1-69	VL1-51	5.9	2.8	28
18	4C11	IgG1λ	CD4i	-	-	-	-	-
19	5D6S	IgG1κ	CD4i	VH1-69	VK3-20	9.3	9.6	26
20	7F11	IgG2κ	CD4i	-	-	-	-	-
21	5E8	IgG2κ	-	-	-	-	-	-
22	7B9N	IgG3κ	-	-	-	-	-	-
23	9F7	IgG1κ	-	-	-	-	-	-
24	39D5	IgG3κ	-	-	-	-	-	-
25	43D7	IgG2κ	-	-	-	-	-	-

VH: Variable heavy chain. VL: Variable light chain. CDRH3: Third complementary determinant region of the heavy chain. Not determine.

antiretroviral treatment. Out of these B cell clones, we identified 25 clones continuously producing MABs reactive to gp120 (Table 1). First, MABs were examined for their reactivity to the V3-peptide corresponding to the V3-region of the gp120_{JR-FL} (NNT20) and the reactive MABs, 0.5 γ , 1D9, 2F8, 3E4, 3G8, 5G2, 717G2 and 16G6, were classified as anti-V3 antibodies. Later, using a set of peptides that have different V3 sequences and overlapping short peptides, we identified the minimum epitope and the cross-reactivity of these antibodies (Supplementary Table 1). The reactivity of these MABs to short peptides was decreased, and only 1D9 and 5G2 bound to 10 mer peptides. Although 2F8 did not recognize any overlapping short peptides, this MAB was capable to bind to the V3 peptide from NSI, correspondent to the CRF01_AE subtype.

MABs other than anti-V3 were classified in three groups according to the effect of soluble CD4 (sCD4) on the reactivity to gp120: CD4bs, CD4i and other epitopes (Figs. 1 and 2). MABs, 0.5 δ , 4E3, 7B5, 42F9, 49G2 and 82D5, were classified as CD4bs antibodies according to the reduction of reactivity in the presence of sCD4. MABs, 4C11, 4E9C, 5D6S, 7F11, 916B2 and 917B11, were classified as CD4i antibodies according to the enhancement effect by sCD4. The rest of MABs, which did not react to the V3 peptide and did not show enhancement or inhibition by sCD4, were classified as MABs to other epitopes. Anti-V3 MAB, KD-247 (Eda et al., 2006a), CD4bs MAB, b12 (Burton et al., 1991) and CD4i MABs, 17b (Thali et al., 1993) were also analyzed as controls.

For the anti-V3 antibodies, no influence in their binding to monomeric gp120 was noted in the presence of sCD4 when analyzed by ELISA (Fig. 1). However, the enhanced reactivity by sCD4 was observed against Env on the cell surface in most of anti-V3 MABs (Fig. 2). This is consistent with the previous reports (Huang et al., 2005; Thali et al., 1993), which showed that the binding of CD4 to gp120 caused the V3 to protrude and became more available, particularly in the strains that use the CCR5 co-receptor. Although a reduction of reactivity was observed for the CD4bs MABs in ELISA, this reduction of reactivity against trimeric Env was not obvious in the MABs, such as 4E3 and 49G2 (Fig. 2).

The enhanced reactivity by sCD4 was observed in all the CD4i MABs, both in ELISA and flow cytometry analysis (Figs. 1 and 2) as previously reported for the CD4i MABs (Lusso et al., 2005; Mbah et al., 2001; Wu et al., 2008). The MABs to other epitopes did not show reactivity to trimeric Env, suggesting that these MABs recognized the unexposed region of the Env trimer (Fig. 2).

Genetic characterization of MABs

Generally, gp120 epitope reactivity is mediated by IgG1, although IgG2 can also be found (Banerjee et al., 2010). MABs predominantly consisted of IgG1. IgG3 was observed only in the "other epitope" group, and none of the antibodies isolated was IgG4 (Table 1). Representative MABs were genetically cloned, and gene usage, somatic mutation percentage and CDRH3 length was determined (Table 1). Anti-V3 antibodies showed a marked preference of the usage of the VH3-30 gene for the variable region of the heavy chain (VH) and VK2-28 for the variable region of the light chain (VL); and only the MAB 16G6 used the VH5-51 gene and λ light chain, which were previously reported as preferential gene usage by anti-V3 antibodies (Gorny et al., 2009). All the anti-V3 antibodies analyzed had the V to I substitution in position 55 (IMGT unique numbering) of FR2 (Supplementary Fig. 1). MABs, 1D9 and 5G2, used the same genes and the length of CDRH3 was also the same among them. These characteristics, as well as the close similarity in their sequences (Supplementary Fig. 1), suggested that these two MABs originated from a common ancestor. In contrast, 0.5 γ , which used the same genes as 1D9 and 5G2, was considered as from another lineage, because 0.5 γ had the CDRH3 different from 1D9 and 5G2 in terms of length and sequences (Table 1 and Supplementary Fig. 1). Two of the three CD4bs MABs used the same genes, VH1-18 and VL1-44, suggesting that these MABs had the same origin. All four of the CD4i MABs analyzed used the VH1-69 gene, which is consistent with previous reports (Gorny et al., 2009; Huang et al., 2004), but did not use the same light chain gene. This indicates that CD4i antibodies with the VH1-69 gene were

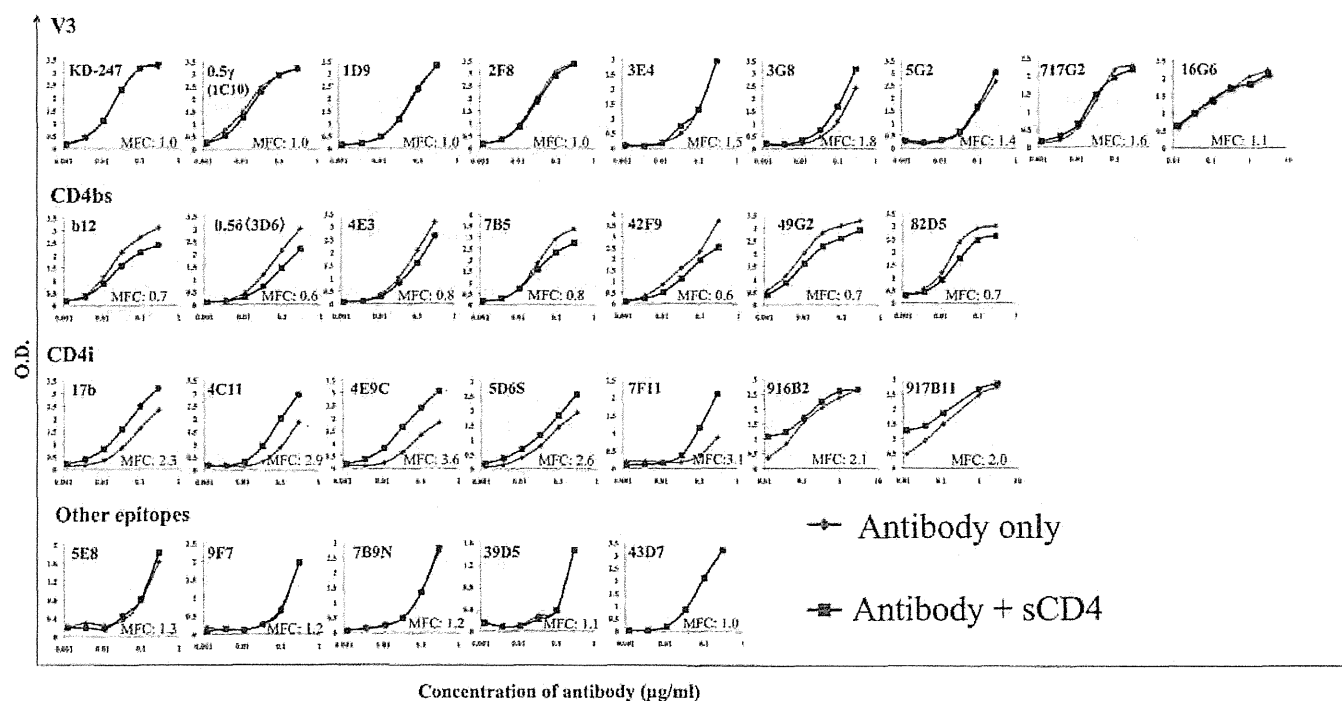


Fig. 1. Effect of sCD4 over binding of MABs isolated from patient KTS376 to monomeric SF2_{gp120}. Reactivity to gp120 was examined for each MAB alone (gray diamond) or in the presence of sCD4 (black square) by capture ELISA assay. No effect was observed for MABs to V3 and "other epitopes". Meanwhile, inhibition of binding was observed for MABs to CD4bs and enhancement of binding was observed for MABs to CD4i epitope. Maximum fold change (MFC) was calculated as follows: O.D. sCD4 positive/ O.D. sCD4 negative.

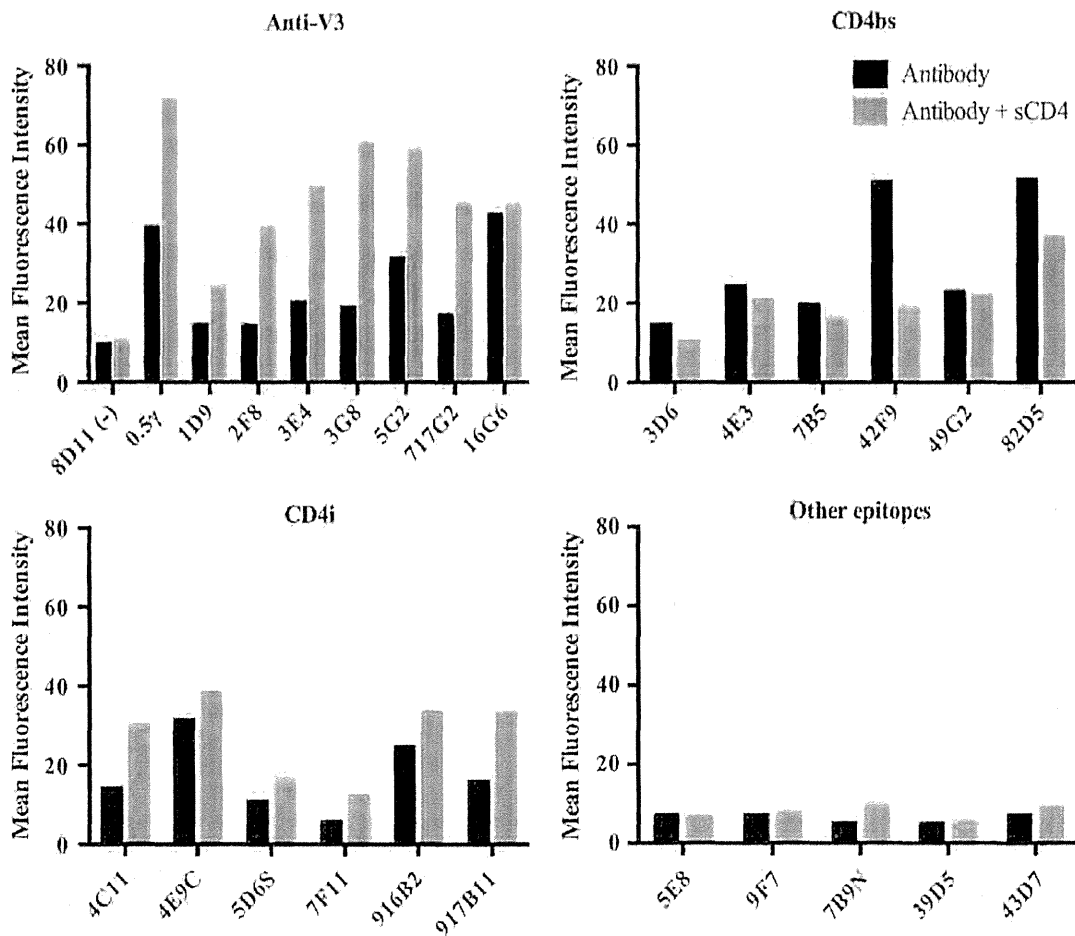


Fig. 2. Binding of MABs from patient KTS376 to Env expressed on the surface of cells. Reactivity to PM1/CCR5 cells chronically infected with HIV-1_{JR-FL} was analyzed using flow cytometer. Mean fluorescence intensity is shown for each MAB in the presence (gray) or absence (black) of sCD4. Enhancement of binding was observed for most of the MABs to V3 and all the CD4i MABs when sCD4 was added. Inhibition of binding was observed for MABs to CD4bs in the presence of sCD4. MABs to other epitopes did not bind to trimeric Env on the cell surface.

frequently induced during infection. Abundance of tyrosines (Y) in CDHR3, which was reported previously in CD4i antibodies (Choe et al., 2003; Huang et al., 2004; Xiang et al., 2002) was present not only in CD4i MABs but also in CD4bs MABs. These results suggest that antibodies with preferential genes were abundantly induced in the patient KTS376, and that dominant antibody lineages were observed in the V3 and CD4bs antibodies.

Mostly, somatic hypermutation percentages were higher in VH than in VL, with the exceptions of 16G6 and 42F9 (Table 1). Overall somatic hypermutation percentages were relatively low (VH mean: 7.9% and VL mean: 4.0%) contrasting with the levels of somatic hypermutations reported for bNABs. For example, mutation percentages of bNABs HJ16, 2G12 and b12 were between 20 and 45% for VH and between 17 and 30% for VL; while the relatively less hypermutated bNABs PG6 and PG9 showed percentages of 21.4% and 18.8% for VH and 21.2% and 14.1% for the VL, respectively (Klein et al., 2013; Sok et al., 2013; Wu et al., 2011; Zhou et al., 2010). The low somatic mutation percentages observed for the MABs isolated from KTS376 corresponded to those reported for the "conventional antibodies" against HIV-1 (Zolla-Pazner, 2014).

Binding activities of the MABs to various HIV-1 Envs

Cross-reactivity of MABs was examined using Envs from various HIV-1 strains (Fig. 3). All the MABs tested bound to Env from most of subtype B viruses including laboratory strains (89.6,

SF162 and YU2) and primary viruses including T/F viruses (WITO and RHPA), 6535.3 (SVPB5) and REJO4541.67 (SVPB16) (Fig. 3). The Env of the laboratory strain, NL4-3, was reactive to all the CD4bs and CD4i MABs, but not to any of the V3 MABs, consistent with the results observed in the V3-peptide ELISA (Supplementary Table 1 and Fig. 3). Cross-subtype binding activities against subtype A, CRF01_AE and subtype C were observed in most of CD4bs and CD4i MABs, while most V3 MABs exhibited significantly lower cross-subtype binding activities than CD4bs and CD4i MABs (Fig. 3, Supplementary Fig. 2). Of the V3 antibodies, 16G6 bound all the subtype C viruses tested, and showed a considerable cross-reactivity compared with other V3 MABs. This is consistent with the previous reports that antibodies encoded by the VH5-51/VL λ genes can recognize Envs from various subtypes (Gorny et al., 2011). These results demonstrated that these MABs isolated from a single patient, as a set of MABs, covered a wide range of viruses including B and other subtypes. The lack of reactivity of some MABs was complemented with the activity of other MABs, and at least two of the three epitopes tested (V3, CD4bs and CD4i) were recognized by these MABs.

Neutralizing activities of the MABs against various HIV-1 subtypes

To evaluate the neutralizing activity of these MABs, we first used representative HIV-1 subtype B laboratory and primary isolates (Fig. 4). The neutralizing activity against SF162 and BaL

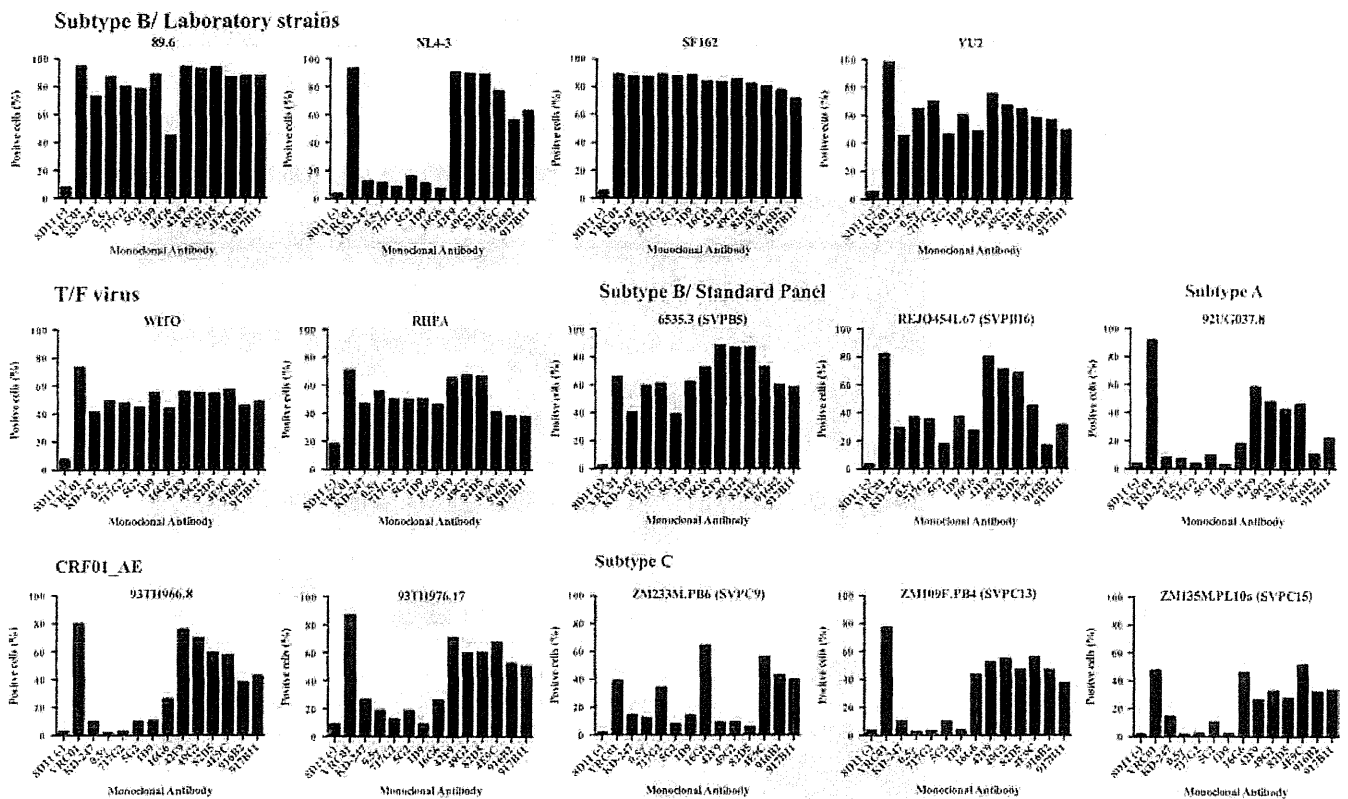


Fig. 3. Cross-reactivity of MAbs from patient KTS376 to Env from various HIV-1 strains. Reactivity to Env from various HIV-1 strains, such as laboratory strains, transmitted/founder (T/F) viruses and viruses belonging to subtype A, B, C and CRF01_AE, was analyzed by flow cytometry using transfected 293T cells. Percentages of cells recognized by MAbs are shown. Controls of the assay included the monoclonal IgG 8D11 (negative control), VRC01 and KD-247 (positive controls). MAbs to V3 potentially bound to cells expressing Envs from all the subtype B viruses tested, with the exception of NL4-3. MAbs to CD4bs and CD4i showed a greater cross-subtype reactivity more than MAbs to V3 MAbs.

was observed for all MAbs tested, consistent with the results of binding activity. Most of the V3 MAbs, with the exception of 16G6, showed a potent neutralization of laboratory strains other than IIB, and 0.5 γ , 717G2 and 1D9 were also effective against primary isolates. Although 16G6 reacted to many viruses (Fig. 3), the neutralizing activity of this MAbs was weak and narrow. The CD4bs and CD4i MAbs neutralized HIV-1 IIB, which was resistant to the neutralization by most of the V3 antibodies because of the two amino acid insertion adjacent to the V3-tip, while the potency and spectrum of the CD4bs and CD4i MAbs were low and narrow, compared with those of V3 MAbs. Especially, KTS376-96, the autologous virus from the patient that MAbs were isolated, was sensitive to V3 MAbs, but not to the CD4i or CD4bs MAbs at all. These results suggest that the V3 antibodies mainly neutralized the viruses present in this patient.

To further evaluate the neutralizing activity of the MAbs, we used a panel of pseudo-typed viruses named standard panel viruses subtype B (SVPB) and C (SVPC) (Li et al., 2006, 2005) (Fig. 4), and one subtype A and two CRF01_AE pseudoviruses. As shown in Fig. 4, 0.5 γ was highly effective against subtype B viruses, and 10 out of 12 SVPB viruses were neutralized by 0.5 γ with a half maximal inhibitory concentration (IC_{50}) below 150 μ g/ml. The coverage of subtype B viruses by 1D9 was lower than for 0.5 γ , but 1D9 showed a cross-subtype neutralization against ZM53M.PB12 (subtype C) and 92UG037.8 (subtype A). Consistent with the results of neutralization of laboratory and primary strains, the potency of CD4bs and CD4i MAbs were low and narrow against standard panel viruses. However, THRO4156.18 (subtype B), which was reported as a neutralizing resistant virus (Li et al., 2005), was neutralized by the CD4bs MAbs 49G2 and 42F9. In addition, TRO.11 (subtype B) and

CAAN5342.A2 (subtype B), which were not neutralized by the V3 MAbs other than 0.5 γ , were sensitive to CD4bs MAbs 49G2 and CD4i MAbs 4E9C, respectively. Moreover, cross-subtype neutralization activity was higher in the CD4bs and CD4i MAbs, which neutralized 4 subtype C viruses, than the V3 MAbs. CD4bs MAbs 49G2 and CD4i MAbs 4E9C significantly contributed to the cross-subtype neutralization, and five out of 12 SVPC viruses (42%) were neutralized by this set of MAbs.

We also evaluated the neutralizing activity of these MAbs against 10 T/F viruses of subtype B (Fig. 4) (Keele et al., 2008; Lee et al., 2009; Ochsenbauer et al., 2012; Salazar-Gonzalez et al., 2009, 2008). Anti-V3 MAbs neutralized 6 out of the 10 analyzed T/F viruses, and CD4i MAbs 49G2 neutralized SUMA, which in contrast to V3 MAbs did not neutralize. Interestingly, 5G2, which showed relatively weak and narrow neutralizing activity against other viruses, showed considerable neutralization against T/F viruses. As a result, MAbs from a single patient provided coverage of 70% of the analyzed T/F viruses.

Plasma from KTS376 obtained in two different time points (2002 and 2005) was able to recapitulate the neutralizing activity of the monoclonal antibodies when confronted with representative viruses from subtype B, C and CRF01_AE (Supplementary Fig. 2).

These results demonstrated that MAbs from patient KTS376 neutralized a broad range of viruses. Although the coverage of each MAbs was limited, in combination they covered a considerable number of viruses from different subtypes and origins. Anti-V3 antibodies mainly provided potency and broadness against viruses inside subtype B, while CD4bs and CD4i MAbs complementarily covered viruses that V3 antibodies did not neutralize, especially non-subtype B viruses.

Viral strain	Sub-type	V3					CD4bs				CD4i			
		KD-247	0.5γ	5G2	717G2	1D9	16G6	0.5δ**	42F9	49G2	82D5	4E9C	916B2	917B11
Laboratory and primary strains														
IIIB	B	16.46	>150	>150	>150	>150	>150	>150	>150	>150	>150	>150	>150	
89.6	B	>150	>150	>150	>150	>150	>150	>150	>150	>150	>150	>150	33.44	
SF162	B	>150	>150	>150	>150	>150	>150	>150	>150	>150	>150	>150	>150	
Bal	B	>150	>150	>150	>150	>150	>150	>150	>150	>150	>150	>150	>150	
JR-FL	B	>150	>150	>150	>150	>150	>150	>150	>150	>150	>150	>150	>150	
YU2	B	12.33	>150	24.8	11.74	>150	13.67	>150	>150	>150	>150	>150	>150	
MOKW	B	>150	>150	>150	>150	>150	>150	>150	>150	>150	>150	>150	>150	
YKI	B	>150	13.78	>150	>150	>150	>150	>150	132.2	15.82	>150	>150	>150	
KKGO	B	>150	>150	>150	>150	>150	>150	>150	>150	>150	>150	>150	>150	
KMT	B	>150	>150	>150	>150	>150	24	59.75	52.24	>150	>150	>150	>150	
KTS376-96*	B	19.03	>150	12.28	12.45	>150	>150	>150	>150	>150	>150	>150	>150	
Standard panel viruses														
6535.3	B	>150	>150	10.1	0.84	25.34	>150	>150	>150	>150	>150	20	34.46	47.49
QH0692.42	B	>150	38	>150	58.6	36.08	>150	>150	>150	>150	>150	>150	>150	>150
SC422661.8	B	>150	>150	>150	>150	>150	>150	>150	>150	>150	>150	>150	>150	>150
PVO.4	B	>150	35	>150	>150	91.19	>150	>150	>150	>150	>150	20	>150	>150
TRO.11	B	>150	82	>150	>150	>150	>150	>150	7.9	>150	>150	>150	>150	>150
AC10.0.29	B	>150	110	>150	>150	>150	>150	>150	>150	>150	>150	>150	>150	>150
RHPA4259.7	B	>150	10.5	>150	59.3	77.4	>150	>150	>150	>150	>150	>150	>150	>150
THRO4156.18	B	>150	>150	>150	>150	>150	>150	71	45	>150	>150	>150	>150	>150
REJO4541.67	B	>150	>150	>150	42	15.43	80.59	30	21	7.3	49.5	>150	>150	38.51
TRJO4551.58	B	17	>150	50	>150	139.4	>150	>150	>150	>150	>150	>150	>150	>150
WITO4160.33	B	28	>150	11.5	51.8	0.4	104.1	>150	>150	>150	>150	>150	>150	>150
CAAN5342.A2	B	>150	80	>150	>150	>150	>150	>150	>150	>150	>150	50	>150	>150
Du156.12	C	>150	>150	>150	>150	>150	>150	>150	>150	NA	>150	>150	>150	>150
Du172.17	C	>150	>150	>150	>150	>150	>150	>150	>150	>150	NA	130.1	>150	>150
Du422.1	C	>150	>150	>150	>150	>150	>150	>150	>150	NA	>150	>150	>150	>150
ZM197M.PB7	C	>150	>150	>150	>150	>150	>150	>150	>150	NA	>150	>150	>150	>150
ZM214M.PL15	C	>150	>150	>150	>150	>150	>150	>150	>150	NA	>150	>150	>150	>150
ZM233M.PB6	C	>150	>150	>150	>150	>150	>150	>150	45	NA	42	10.26	>150	>150
ZM249M.PL1	C	>150	>150	>150	>150	>150	>150	>150	>150	NA	>150	>150	>150	>150
ZM53M.PB12	C	>150	>150	>150	>150	>150	>150	>150	>150	NA	>150	>150	>150	>150
ZM109F.PB4	C	>150	>150	>150	>150	>150	>150	55	>150	45	NA	42	35.01	48.65
ZM135M.PL10a	C	>150	>150	>150	>150	>150	>150	>150	>150	28	NA	>150	>150	>150
CAP45.2.00.G3	C	>150	>150	>150	>150	>150	>150	>150	>150	>150	NA	>150	>150	>150
CAP210.2.00.E8	C	>150	>150	>150	>150	>150	>150	>150	>150	>150	NA	>150	>150	>150
92UG037.8	A	>150	>150	>150	>150	76.86	>150	NA	>150	>150	>150	>150	>150	>150
93TH966.8	CRF01_AE	>150	>150	>150	>150	>150	>150	NA	>150	>150	>150	>150	>150	>150
93TH976.17	CRF01_AE	>150	>150	>150	>150	>150	>150	NA	>150	>150	>150	>150	>150	>150
Transmitted/Founder viruses														
WITO	B	>150	147.1	>150	>150	43.02	>150	NA	NA	>150	>150	>150	>150	>150
CH058	B	>150	62.86	84.67	126.65	25.19	>150	NA	NA	>150	>150	>150	>150	>150
RHPA	B	98.98	74.38	99.3	>150	>150	>150	NA	NA	>150	>150	>150	>150	>150
REJO	B	>150	>150	>150	>150	20.1	>150	NA	NA	>150	>150	>150	>150	>150
TRJO	B	>150	>150	>150	>150	>150	>150	NA	NA	>150	>150	>150	>150	>150
CH106	B	>150	>150	>150	>150	>150	>150	NA	NA	>150	>150	>150	>150	>150
CH077	B	>150	>150	16.23	>150	>150	>150	NA	NA	>150	>150	>150	>150	>150
SUMA	B	>150	>150	>150	>150	>150	>150	NA	NA	136.33	>150	>150	>150	>150
CH040	B	>150	>150	>150	>150	>150	58.4	NA	NA	>150	>150	>150	>150	>150
THRO	B	>150	>150	>150	>150	>150	>150	NA	NA	>150	>150	>150	>150	>150

Fig. 4. IC₅₀ (μg/ml) of MAbs from KTS376 against strains of HIV-1 using TZM-bl cells and single-round infection assay. The autologous virus (KTS376-96) was analyzed together with other laboratory and primary strains. Analysis of laboratory and primary strains for 0.5δ was performed using the MTT assay of supernatant of infected PM1/CCR5 cells. Not available results are denoted as NA. Color code is as follows: Red: IC₅₀ 0.05–10; Orange: IC₅₀ > 10–50; Yellow: IC₅₀ > 50–150 μg/ml.

Synergistic effects of anti-V3 and CD4bs antibodies against HIV-1

Recent studies on functional trimers of envelopes suggest that exposure of V3-epitope and coreceptor binding sites including the CD4i epitope occurs following the interaction of gp120 with CD4 (Kwong et al., 2002, 1998; Liu et al., 2008; Mbah et al., 2001). In fact, sCD4-mediated enhancement was observed in the V3 and CD4i MABs (Fig. 2), as has been previously reported (Lusso et al., 2005; Thali et al., 1993; Wu et al., 2008). We then tested whether antibodies to CD4bs have the capacity to alter the envelope conformation and induce some critical epitopes accessible for the antibodies of other specificities. We first tested the binding activity of MABs in the presence or absence of the CD4bs MAB 0.5δ by ELISA (Fig. 5). Marked enhancement of binding of 0.5γ was observed in the presence of 0.5δ. The enhancement was also observed for the other V3 antibody 3E4, although the effect was much higher in 0.5γ than in 3E4. In contrast, suppression in the binding of 0.5δ itself and CD4i MAB 4C11 was observed in the presence of 0.5δ. This suggests that the 0.5δ epitope may overlap with that of 4C11, or that the binding of either MAB may interfere with the other sterically.

Then, we tested the effect of MABs combinations, such as 0.5γ (V3) and 0.5δ (CD4bs), 1D9 (V3) and 49G2 (CD4i), and 16G6 (V3) and 17G2 (V3) over neutralization. The combinations of MABs showed an additive effect in most of cases, while the combination of 0.5γ and 0.5δ showed a synergistic effect in the neutralizing activity of HIV-1_{JR-FL} (Fig. 6). The combination of these MABs was shown to be more effective than either MAB alone and the synergy of neutralizing activity observed for the combination of 0.5γ and

0.5δ was up to 25% (Supplementary Table 3). This result suggests that these antibodies, besides their complementarity, can act synergistically. This phenomenon of synergism and complementarity may play an important role “in vivo” for suppressing viruses in a patient.

ADCC activities of the MABs

It has been reported that antibodies contribute to protection by its effector-mediated functions such as ADCC (Haynes et al., 2012a; Liao et al., 2013; Xiao et al., 2010). Then, we determined the ADCC activities of MABs from patient KTS376. First, we analyzed cells coated with gp120 from SF2 and cells infected with BaL and YU2 (Fig. 7, Supplementary Fig. 3). Significant ADCC activity was observed in most of the MABs from the three groups. The CD4i MAB 916B2 showed neutralizing activity against BaL, but did not show any statistically significant ADCC activity against BaL. The 916B2 epitope may require the CD4 binding to Env, as reported previously (Veillette et al., 2014). ADCC activity of MABs from patient KTS376 was also evaluated against cells infected with five T/F virus strains (Fig. 8, Supplementary Fig. 4). ADCC activity for the T/F viruses was relatively weak compared with the response observed for gp120, BaL and YU2. THRO was sensitive to all the MABs tested, while ADCC activity against CH106 was statistically significant in CD4bs MAB 49G2. Interestingly, the V3 MABs acted complementarily against CH040 and REJO. ADCC activity against CH040 was observed in MABs, 0.5γ and 16G6, and the other V3 MABs were effective against REJO. Despite the fact that no neutralizing activity was observed for THRO, all the MABs showed

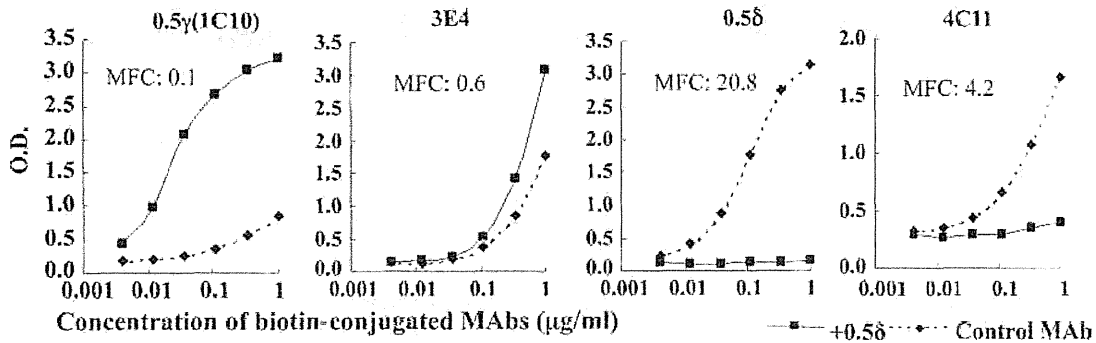


Fig. 5. Effect of CD4bs MAB 0.5δ on reactivity of other MABs. Reactivity of MABs was analyzed by ELISA for biotin conjugated antibody alone (dotted line) or in combination with 0.5δ (solid line). Marked enhancement of reactivity in the presence of 0.5δ was observed in the MAB to V3 0.5γ. Another anti-V3 MAB 3E4 showed only a slight enhancement by 0.5δ, and abrogation of reactivity was evident for 0.5δ and 4C11. Maximum fold change (MFC) was calculated as follows: O.D. 0.5δpositive/ O.D. 0.5δ negative.

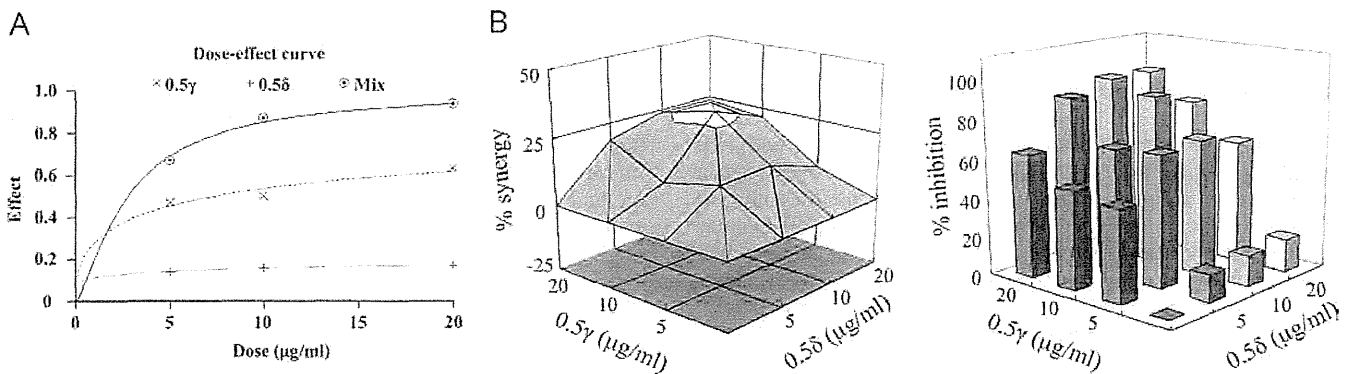


Fig. 6. Synergistic neutralizing activity of the anti-V3 MAB 0.5γ and the CD4bs MAB 0.5δ. Neutralization activity of 0.5γ alone (X symbol), 0.5δ alone (+ symbol) and 1:1 combination of both MABs (Circle and dot symbol) was evaluated and is shown as a dose-effect curve (A). The percentages of synergy (B) and viral inhibition (C) reached by combinations of 0.5γ and 0.5δ are shown. Neutralizing activity was analyzed against HIV-1_{JR-FL}. Synergy between 0.5γ and 0.5δ was calculated using the Chou–Talalay method and 3 dimensional analyses.

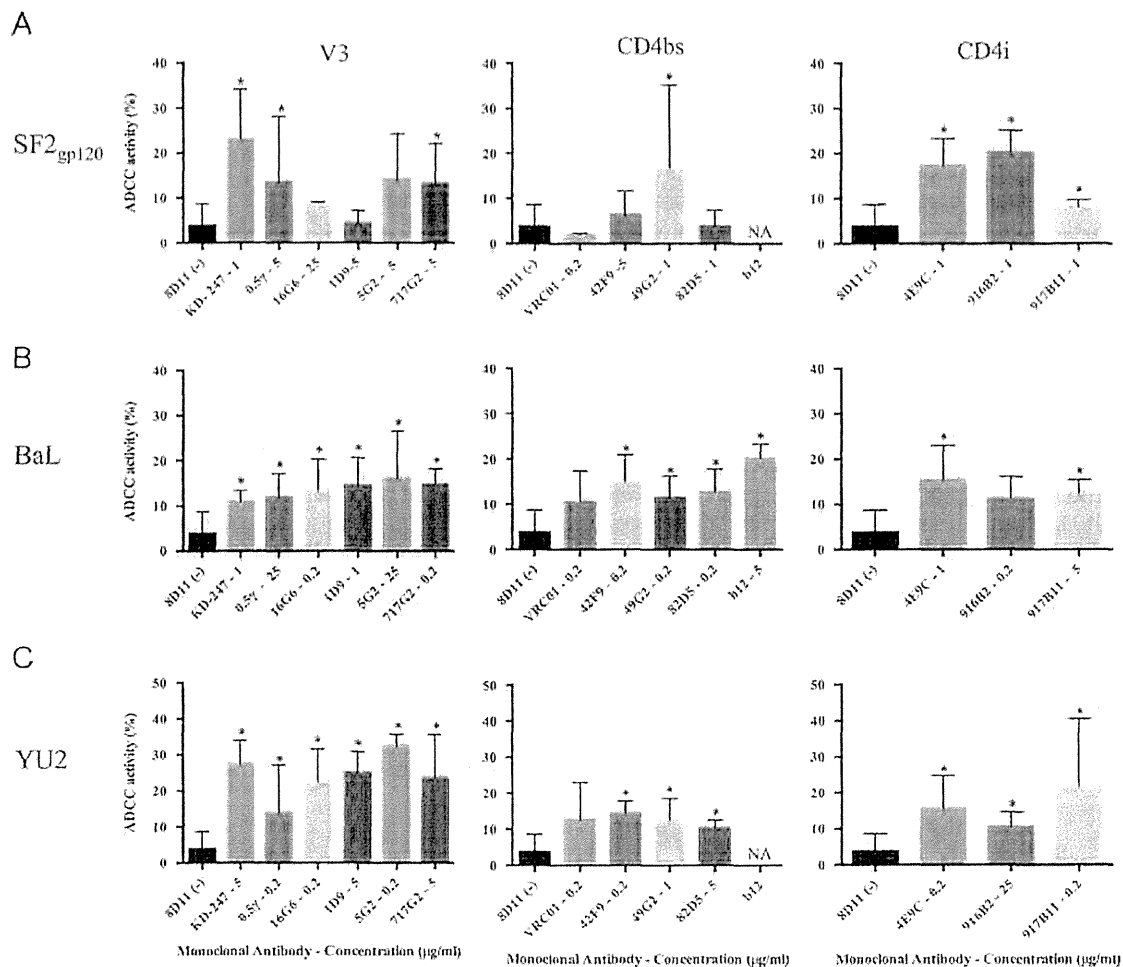


Fig. 7. ADCC activity of MAb against CEM.NKr.CCR5 cells coated with SF2_{gp120} (A), infected with BaL (B) and YU2 (C). ADCC activity was evaluated using CEM.NKr.CCR5 cells stained with CFSE and PKH-26 as target cells and PBMC (A and C) or NK-enriched PBMC (B) from healthy donors as effector cells. MAb concentration between 0.2 and 25 $\mu\text{g/ml}$ was analyzed, and the maximum percentages of killing are shown for each MAb. Concentration of MAb ($\mu\text{g/ml}$) is indicated together with MAb name. Asterisks correspond to values statistically different from the negative control ($p < 0.05$) calculated with the Mann-Whitney U test.

significant ADCC activity against this virus. This indicates that ADCC activity is not correlated with neutralizing activity. However, CH106 was resistant to both neutralization and ADCC.

These results demonstrated that MABs from a single donor presented ADCC activity against HIV-1 strains including T/F viruses. The coverage of a wide range of HIV-1 strains by ADCC supports the complementary character of these MABs from a single patient, not only for the neutralizing activities, but also for the non-neutralizing activities.

Presence of KTS376-like antibodies in plasma samples

In order to determine the presence of antibodies with the specificity similar to the MABs from patient KTS376, plasma samples from various patients were examined for the ability to block binding of 0.5 γ , 3E4, 0.5 δ and 4C11 (Fig. 9, Supplementary Fig. 5). Plasma samples from HIV-1-infected patients, which included progressors ($N=47$), slow progressors ($N=25$), long-term non-progressors, LTNP ($N=20$) and non-B-infected ($N=11$) patients, significantly suppressed the binding of CD4bs MAb 0.5 δ and CD4i MAb 4C11. This is consistent with a previous observation that most of the patients have antibodies to CD4bs and CD4i (Binley et al., 2008; Dhillion et al., 2007; Gnanakaran et al., 2010; Moulard et al., 2002; Sather et al., 2009). The V3 MABs, 0.5 γ and 3E4, were not inhibited significantly by plasma samples from non-

B-infected patients, and this maybe due to the poor cross-subtype reactivity of the V3 MABs (Fig. 3). Disease progression was associated with the low inhibition of MABs, and the plasma samples from progressors inhibited the binding of MABs less strongly than those from LTNP. Accordingly, the inhibition of 0.5 γ , which was weakly inhibited by plasma samples compared with other MABs, was not significant in progressors. However, considerably longer times of infection in the long-term non-progressor and the slow progressor groups may have contributed to affinity maturation of antibodies in these groups. This suggests that the presence of antibodies similar to those in patient KTS376 may contribute to the control of HIV-1 infection. On the other hand, KTS376-like antibodies were found in most of HIV-1-infected patients regardless of their disease status, suggesting that antibodies against V3, CD4bs and CD4i were induced in most HIV-1-infected patients similarly to patient KTS376.

Discussion

In the present study, we isolated 25 MABs from a patient, KTS376, who had suppressed HIV-1 infection for more than 25 years without any treatment, and further analyzed these MABs to clarify the mechanism to controlling HIV-1 infection. A wide coverage of viruses by a set of monoclonal antibodies from

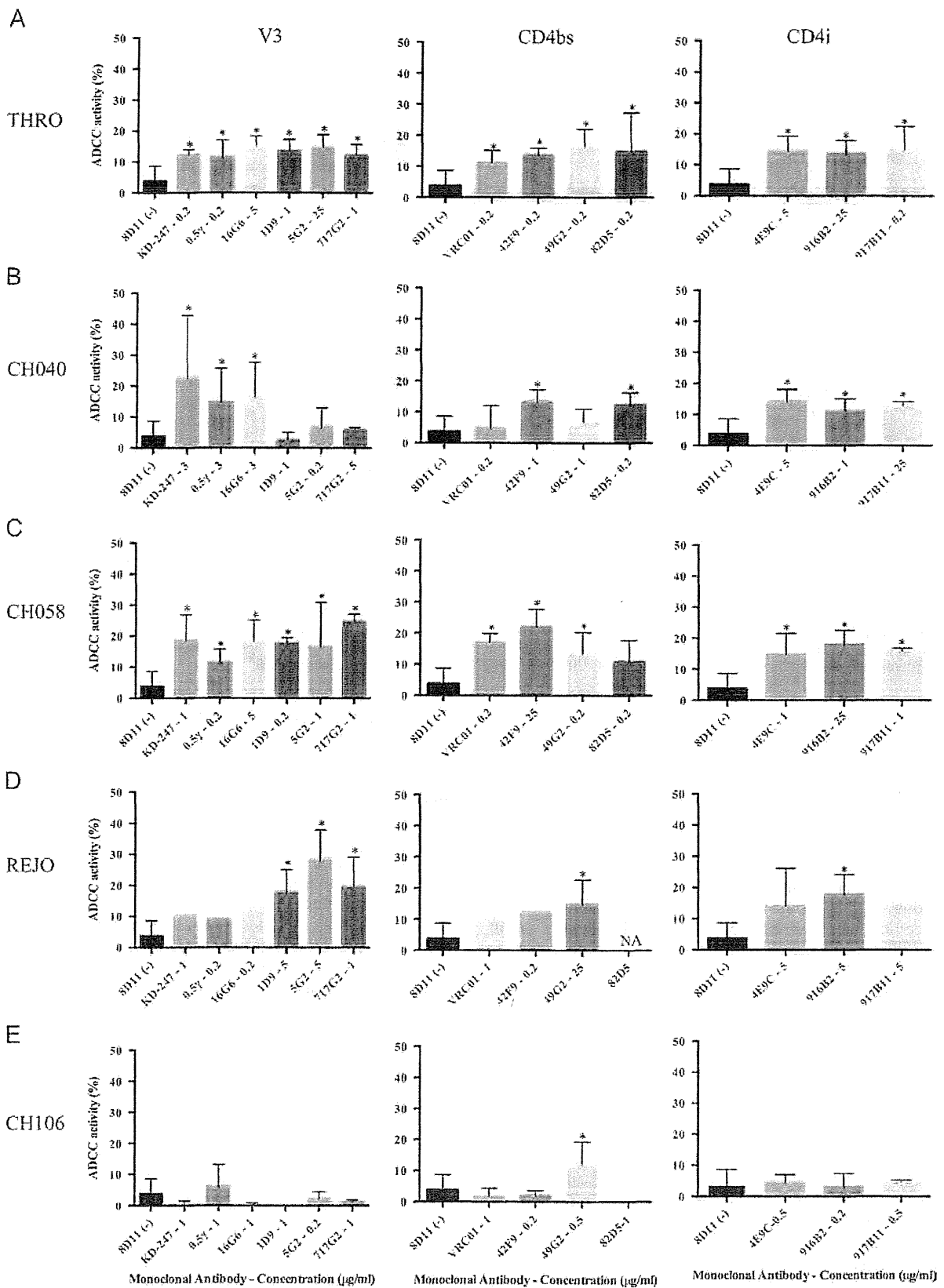


Fig. 8. ADCC activity of MAb against CEM.NKr.CCR5 cells infected with T/F viruses, THRO (A), CH040 (B) CH058 (C) REJO (D) and CH106 (E). ADCC activity was evaluated using CEM.NKr.CCR5 cells stained with CFSE and PKH-26 as target cells and PBMC (C, D and E) or NK-enriched PBMC (A and B) from healthy donors as effector cells. MAb concentration between 0.2 and 25 µg/ml was analyzed, and the maximum percentages of killing are shown for each MAb. Concentration of MAb (µg/ml) is indicated together with MAB name. Asterisks correspond to values statistically different from the negative control ($p < 0.05$) calculated with the Mann-Whitney *U* test.

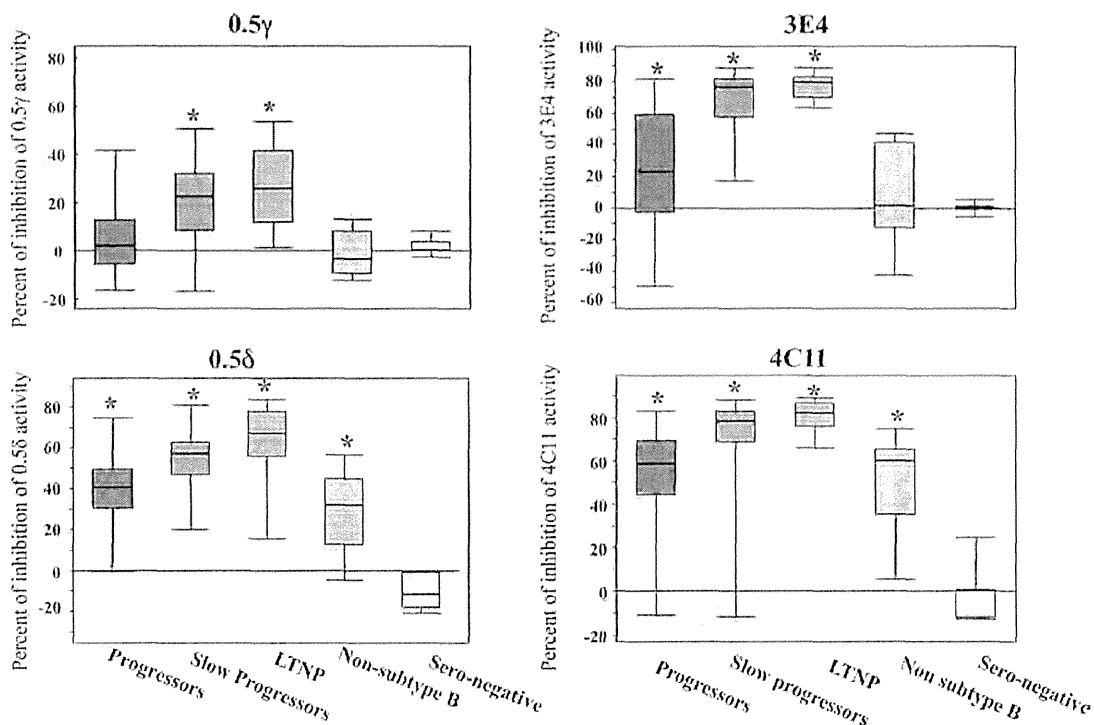


Fig. 9. Induction of antibodies with the specificity similar to MAbs from KTS376 in HIV-1-infected patients. Competition ELISA was performed using biotin-conjugated MAbs, 0.5γ, 3E8, 0.5δ and 4C11, and plasma samples (1:50 dilution) as a competitor. Plasma samples were obtained from progressors ($N=47$), slow progressors ($N=25$), Long-term non-progressors (LTNP, $N=20$), Non-subtype B infection ($N=11$) and sero-negative ($N=7$) individuals. Asterisks correspond to values statistically different from those of sero-negative individuals ($p < 0.05$) calculated by Student's *t*-test. The estimated time of infection with HIV-1 of patients from the long-term non-progressor group and the slow progressor group were 23 and 15 year, respectively. Time of infection for the other groups is not available.

KTS376 suggests that the humoral response played an important role in the long-term suppression of the patient. However, we cannot rule out other mechanisms, such as cellular response and viral fitness. The moderate neutralizing potency and breadth indicates that these MAbs are not classified as broad neutralizing antibodies, but rather as “conventional antibodies”. This type of antibodies was recently described by Zolla-Pazner, as antibodies that have limited breadth and potency in standard neutralization assays and are commonly induced in HIV-1-infected patients. Conventional antibodies are frequently elicited during infection, and induced by many vaccine candidates tested to date, but none have yet induced broadly reactive neutralizing antibodies (Zolla-Pazner, 2014). Although each conventional antibody has only a limited breadth in neutralization, the considerable cross-reactivity of MAbs from patient KTS376, indicates that conventional antibodies can cover a wide range of viruses.

Anti-V3 MAbs had the higher frequency and potency of neutralizing activity when compared with MAbs from other specificity, especially against subtype B viruses. V3 is highly immunogenic and it is estimated that about half of the antibody responses against HIV-1 Env in patient serum is directed against this region (Javaherian et al., 1989; Moore et al., 1994; Zolla-Pazner, 2004) and at a sequence level, V3 is more conserved in comparison with the other variable regions of gp120 (Jiang et al., 2010). The anti-V3 MAbs 0.5γ and 1D9 showed the broadest neutralizing activities, comparable to that of other anti-V3 MAbs with cross-reactivity, as previously reported (Andrabi et al., 2013). MAb 16G6 has a remarkable cross-binding activity, consistent with reports of anti-V3 antibodies derived from the VH5-51 gene (Gorny et al., 2011). However, 16G6 has a weak neutralizing activity and this may be related with its low somatic mutation percentage. Despite the fact that anti-V3 MAbs frequently depend on the “GPGR” motif in the V3 tip, viruses with a different motif,

such as CH040 (GPGQ) and CH077 (GALR), were neutralized by these V3 MAbs. The induction of such antibodies with a relatively broad reactivity may require new approaches for designing V3-scaffold immunogens and adjuvants based on previous observations (Zolla-Pazner et al., 2011). In addition, the high frequency of 0.5γ-like antibodies in LTNP suggests that maturation of B cells, which is much shorter than those for bNAbs, may be important to induce V3 antibodies with cross-reactivity.

CD4bs MAbs are reported as the earliest cross-neutralizing response in patients (Andrabi et al., 2013; Jiang et al., 2010; Zolla-Pazner et al., 2011) and is not rare to find them in HIV patients' sera. Patient KTS376 was not the exception and several CD4bs MAbs with cross-neutralizing activity, even against non-B subtype viruses, were isolated. However, as it is also observed for antibodies other than CD4bs, higher concentration of antibody was required for efficient neutralization. These types of antibodies could also contribute to enhancing the V3 MAbs response, as was observed when the anti-V3 0.5γ was combined with the CD4bs MAb 0.5δ, showing the complementary and synergistic potential of CD4bs MAb. Synergy of antibodies was reported to contribute to HIV-1 control in a vaccine study (Pollara et al., 2014), and in this study we showed that synergy was also observed in a combination of antibodies derived from a single donor. This suggests that this synergy phenomenon can contribute to suppression of HIV-1 in vivo.

CD4i MAbs are induced quite frequently in HIV-1-infected patients (Decker et al., 2005). CD4i MAbs isolated from patient KTS376 were not as potent as the V3 MAbs, but were able to neutralize viruses that were not covered by anti-V3 and CD4bs MAbs; thus providing a complementarity to the antibody set. Identification of at least four lineages of CD4i antibodies, which were revealed from a genetic analysis of light chain genes, indicates the vigorous induction of CD4i antibodies in this patient.

CD4i antibodies may not contribute significantly to protection from HIV-1 infection, but may play an important role in controlling HIV-1 replication after HIV-1 infection. Some CD4i antibodies bound to a hybrid epitope conformed by the CD4 and the gp120, and for these antibodies, the presence of CD4 is indispensable for binding (Lewis et al., 2011). However, our MABs were able to bind to gp120 even without CD4, which suggests that some part of the epitope may be exposed even before binding to CD4.

Low somatic hypermutation rates of MABs from patient KTS376 contrasts with those of the bNABs. A high mutation percentage is a consequence of the affinity maturation of antibodies, and is one of the main obstacles for induction of bNABs by vaccination. In fact, a positive correlation between the level of somatic hypermutation and the development of strength and breadth of the neutralizing activity of an antibody was reported (Sok et al., 2013). However, our data show that MABs even with low levels of affinity maturation are capable of binding and neutralizing a wide range of viruses, when antibodies targeting V3, CD4bs and CD4i acted complementarily and we observed also synergy. Synergy of neutralizing activity by two antibodies with different specificity has been already reported. Pollara et al. (2014) recently showed that C1 and V2 monoclonal antibodies isolated from RV144 vaccinees have synergistic activities for neutralization, infectious virus capture, and ADCC, and proposed that synergy among antibodies with different epitope specificities contributes to HIV-1 antiviral antibody responses. Although it is difficult to compare our results with the results reported by them due to the use of different experimental settings, they showed a 20- to 65-fold decrease of IC₅₀s by combination of antibodies.

Besides neutralizing activity of the antibodies, ADCC activity has been reported to have great importance in the protection and control of the HIV-1 infection (Haynes et al., 2012a; Rerks-Ngarm et al., 2009; Wren et al., 2012). Antibodies with ADCC activity tend to have cross- or broad- activity (Smalls-Mantey et al., 2012). In addition, ADCC-mediated natural killer cell activation was significantly broader and stronger in HIV controllers than in HIV progressors (Madhavi et al., 2014). We showed significant ADCC activities of MABs against various viruses, especially T/F viruses. The *in vitro* evaluation of ADCC presents certain obstacles, and one of them is a lack of suitable target cells. We used CEM.NKr.CCR5 cells as target cells, but the susceptibility of these cells to HIV-1 infection is not high due to the presence of restriction factors (Han et al., 2008). This limited the number of primary isolates evaluated, because infections could not be established for many viruses. The factors behind the presence or magnitude of the ADCC responses are not fully understood. It was reported that neutralizing and gp120 titers did not predict ADCC activity (Alpert et al., 2012). Although binding to Env is necessary for ADCC activity, we cannot observe a correlation between these two factors. Interaction of gp120 with CD4 was shown to changed ADCC activity (Veillette et al., 2014) and this could have important implications for the conformational status of Env in the infected cells. Possible causes may include the interactions between epitope and paratope and the differences in the level of epitope expression required for ADCC activity. However, the exact reasons behind this lack of correlation among binding, neutralizing and ADCC activities remains unclear, and will be a topic of future research.

A wide coverage of HIV-1 viruses by bNABs has been previously reported (Walker et al., 2011) and great effort is invested in developing this type of antibodies by vaccination (Zolla-Pazner, 2014); however, this study supports the rationale that “conventional antibodies” are capable to provide considerable levels of coverage, as we observed that the antibodies derived from a single patient had complementary and synergistic neutralizing activity and ADCC activity. The use of mixture of Env had been proposed as

a way to achieve the induction of polyclonal response in animal models (Nkolola et al., 2014; Seaman et al., 2007, 2005). Although the induction of antibodies to specific epitopes will require further studies, antibody induction to a specific epitope was demonstrated using the antigen containing epitope with scaffold (Zolla-Pazner et al., 2011). Elicitation of antibodies with characteristics similar to MABs from this patient, which is much easier than elicitation of highly mutated bNABs, could be a strategy for developing an effective vaccine against HIV-1.

Material and methods

Study participant

B cells were isolated from patient KTS376. During the period of B cell isolation, CD4 cells count was above 200/ μ l (mean of 17 visits; 297/ μ l) and viral load was below 200 copies/ml (mean of 17 visits; 44.3 copies/ml), and the time frame corresponded to 23 to 28 years after infection with HIV-1. Also, KTS376 did not receive any antiretroviral treatment and besides having Hepatitis C virus co-infection, did not present any symptoms or signs of immunodeficiency. Human blood samples were collected from KTS376 after signed informed consent in accordance with the study protocol and informed consent was reviewed and approved by the Ethics committee for clinical research & advanced medical technology at the Kumamoto University Medical School.

Cells, reagents and viruses

TZM-bl (Derdeyn et al., 2000; Lambotte et al., 2009; Platt et al., 1998; Takeuchi et al., 2008; Wei et al., 2002), 293A (Life Technologies, Carlsbad, CA) and 293T (Graham et al., 1977) cells were maintained in Dubelcco's modified Eagle medium (DMEM; Sigma, St. Louis, MO) and supplemented with 10% heat-inactivated fetal calf serum (FCS; Thermo Scientific, Waltham, MA). CEM.NKr.CCR5 cells (Howell et al., 1985; Lyerly et al., 1987; Trkola et al., 1999) were maintained in RPMI-1640 medium (Sigma, St. Luis MO) supplemented with 10% FCS. PM1/CCR5 cells (Monde et al., 2007) were maintained in RPMI-1640 supplemented with 10% FCS and 100 μ g/ml of G418 sulfate (Calbiochem-EMD Millipore, Billerica, MA). PM1/CCR5 cells chronically infected with HIV-1_{JR-FL} were maintained in RPMI-1640 supplemented with 10% FCS. Recombinant human soluble CD4 (sCD4) was purchased from R&D systems (Minneapolis, MN). The primary HIV-1 strains, MOKW, YKI, KKGO, KMT and KTS376-96 were isolated from drug-naïve Japanese patients (Maeda et al., 2001). These viruses were passaged in phytohemagglutinin (PHA)-activated peripheral blood mononuclear cells (PBMCs) and the culture supernatant was stored at -80°C until use. KD-247, an anti-V3 humanized mouse antibody, was produced by transferring the complementary region genes from the mouse hybridoma clone C25 into genes of the human V region as previously described (Eda et al., 2006b). CD4i MAb 17b was a kind gift from J. Robinson (Department of Pediatrics, Tulane University Medical Center, New Orleans, LA). CD4bs VRC01 was produced by Freestyle 293 expression system (Invitrogen, Life Technologies, Carlsbad, CA). Env plasmids of the Standard Virus Panel for subtype B and C strains (Li et al., 2006, 2005) were used for pseudovirus preparation and flow cytometry analysis. TZM-bl cells, CEM.NKr.CCR5 cells, VRC01 plasmid, SPVB and SPVC Env plasmids, and T/F plasmids were obtained through the NIH AIDS Reagent program, Division of AIDS, NIAID, NIH, by the kind contribution from Dr. John C. Kappes, Dr. Xiaoyun Wu, Tranzyme Inc., Dr. D. Montefiori, Dr. F. Gao, and Dr. Christina Ochsenbauer.

Pseudovirus and infectious molecular clones preparation

Pseudoviruses were prepared by transfecting exponentially dividing 293T cells with 5 µg of *rev/env* expression plasmid and 10 µg of an *env*-deficient HIV-1 backbone vector (pSG3ΔEnv), using Lipofectamin 2000 transfection reagent (Invitrogen, Life Technologies, Carlsbad, CA). Pseudovirus-containing culture supernatants were harvested 48 h after transfection, filtered (0.45 µm), and stored at –80 °C until use. Plasmids from the transmitted/founder viruses pWITO.c/2474, pCH058.c/2960, pRHPA.c/2635, pREJO.c/2864, pTRJO.c/2851, pCH106.c/2633, pCH040.c/2625, pCH077.t/2627, pSUMA.c/2821, and pTHRO.c/2626 (Keele et al., 2008; Lee et al., 2009; Salazar-Gonzalez et al., 2009, 2008) were used for producing infectious molecular clones by transfecting 5 µg of plasmid to 293T cells as described above.

Monoclonal antibody isolation

Transformation of B-cells with Epstein-Barr virus (EBV) and subsequent cloning were performed as previously described elsewhere (Matsushita et al., 1986). PBMC were separated from a patient with hemophilia A (KTS376) who had been infected with HIV-1 for more than 25 years without any antiretroviral treatment, by density gradient centrifugation of heparinized blood using Ficoll-paque (GE Healthcare, Cleveland, OH). Supernatants from individual clones was screened for the presence of IgG antibody that binds to the monomeric SF2 gp120 in a gp120 capture assay (Moore et al., 1994). Briefly, gp120 from SF2 (Austral Biologicals, San Ramon, CA) was captured onto solid phase via their carboxyl termini using sheep polyclonal antibody D7324 (Aalto Bioreagents, Dublin, Ireland). Supernatant samples were added to wells and IgG bound to gp120 was detected with alkaline phosphatase-conjugated goat anti-human IgG (Sigma, St. Luis MO) followed by addition of phosphatase substrate (Sigma, St. Luis MO). A₄₀₅ measurements were taken using a microplate reader (Biorad, Hercules, CA).

Construction of recombinant IgG

Recombinant IgG from antibodies 16G6, 1D9 and 7171G2 were constructed as described some lines below, and used exclusively in the posterior analysis. RNA was extracted from B cells of interest with the RNeasy mini kit (Qiagen, Venlo, Netherlands). First-strand cDNA was synthesized using oligo(dT)20 (Toyobo, Osaka, Japan) and the SuperScript III Reverse transcriptase (Invitrogen, Life Technologies, Carlsbad, CA). The heavy chain variable regions were amplified using the following primers, LH1 (5'-TGG TGG CAG CCA CCG GTG CCC ACT CCC AGG TGC AG-3'), LH3 (5'-TGG TGG CAG CCA CCG GTG TCC AGT GTG ARG TGC AG-3'), LH46 (5'-TGG TGG CAG CCA CCC GGG TCC TGT CCC AGG TGC AG-3'), LH5 (5'-TGG TGG CAG CCA CCG GAG TCT GTT CCG AGG TGC AG-3') and APS-R (5'-GGG GGA AGA CCG ATG GGC-3'). The light chain κ variable regions were amplified using primers, GKV1 (5'-GGT GCC TAC GGG GAT ATC CAG ATG ACC CAG TCT CC-3'), GKV24 (5'-GGT GCC TAC GGG GAT ATT GTG ATG ACY CAG TCT CC-3'), GKV3 (5'-GGT GCC TAC GGG GAT ATT GTG WTG ACR CAG TCT CC-3'), GKV5 (5'-GGT GCC TAC GGG GAT ACG ACA CTC ACG CAG TCT CC-3') and HCK5-B (5'-GAA GAC AGA TGG TGC AGC CAC AGT-3'). The light chain λ variable regions were amplified using primers, LLS1 (5'-ACT TTC TGC ACA GGC TCC TGG GCC CAG TCT GTG CTG-3'), LLS2 (5'-ACT TTC TGC ACA GGC TCC TGG GCC CAG TCT GCC CTG-3'), LLS3 (5'-ACT TTC TGC ACA GGC TCT GTG ACC TCC TAT GAG CTG-3'), LLS45 (5'-ACT TTC TGC ACA GGC TCT CTC TCS CAG CYT GTG CTG-3'), LLS6 (5'-ACT TTC TGC ACA GGC TCT TGG GCC AAT TTT ATG CTG-3'), LLS7 (5'-ACT TTC TGC ACA GGC TCT AAT TAY CAG GCT GTG CTG-3'), LLS8 (5'-ACT TTC TGC ACA GGC GTG GAT TCT CAG

ACT GTG GTG-3') and VL-R (5'-CAG TGT GGC CTT GTT GGC TTG-3'). Polymerase chain reaction (PCR) was performed using the following conditions by Platinum Taq DNA Polymerase High Fidelity (Invitrogen, Life Technologies, Carlsbad, CA): 94 °C for 30 s, followed by 35 cycles of 94 °C for 15 s, 55 °C for 15 s, and 68 °C for 60 s. The PCR products of the heavy chain, light chain κ and light chain λ were cloned into vectors plgGH, pKVA2 and pLSH, respectively, using the GeneArt Seamless Cloning and Assembly kit (Invitrogen, Life Technologies, Carlsbad, CA). The vector plgGH was basically constructed from plgG (Rader et al., 2002), pHCG (Kuwata et al., 2011) and the plasmid to produce MAb 1C10 (0.5γ) heavy chain fragment. Briefly, the VH gene was amplified from a B cell line producing MAb 1C10 with primers HFabVH3a-F and HFabVHJb-B (Barbas et al., 2001). The CH1 region was amplified using pCOMB3XTT and primers, HlgGCH1-F and dpseq (Barbas et al., 2001). These PCR products were combined by PCR with primers SgrVH135F (5'-GCC ACC GGT GCC CAC TCC SAG GTG CAG CTG KTG-3') and dsp-R (5'-CAG TTT AAA CCT AAG AAG CGT AGT CCG GAA C-3'). The connected PCR product was digested with *SgrAI* and *Apal* and inserted into pHCG. The resulting p1C10Fab produced the 1C10 heavy chain fragment. The *XbaI*-*Apal* fragment from pCOMB3XSS and the *Apal*-*PmeI* fragment from the PCR product, which was amplified using primers, HlgGH1-F (5'-GCC TCC ACC AAG GGC CCA TCG GTC-3') and CH-R (5'-AGG TTT ACT AGT ACC ACC ACA TGT TTT TAT CTC-3'), and plgG as a template, were inserted into p1C10Fab. The resultant plgGH has the signal peptide region and the constant regions of IgG, and was used to clone VH genes after removing the stuffer sequence by digestion with *SgrAI* and *Apal*. The vector pKVA2 was constructed by insertion of two PCR products into pcDNA3.1/Hygro(+) (Invitrogen, Life Technologies, Carlsbad, CA) and was used to clone VK genes after digestion with *EcoRV* and *AfeI*. The signal peptide region was amplified using the primers, SPKNH-F (5'-AAG CTA GCA TGG TGT TGC AGA C-3') and SPKEV-R (5'-AAG ATA TCC CCG TAG GCA CCA GAG-3'), and plgG as a template, and the *NheI*-*EcoRV* fragment was used for the insertion. The light chain κ constant region was amplified using the primers, EcVAfe-F (5'-CCG ATA TCT TAG CGC TGC ACC ATC TGT CTT C-3') and BGH-R (5'-TAG AAG GCA CAG TCG AGG-3'), and p1C10L, which had the *HindIII*-*XbaI* fragment containing MAb 1C10 light chain in pcDNA3.1/Hygro(+). The vector pLSH was constructed by inserting the *HindIII*-*HpaI* fragment and the *HpaI*-*XbaI* fragment, which were amplified using p916B2L and primer pairs, T7-F and HpaSfo-R, and Hpa-F and BGH-R, respectively, into pcDNA3.1/Hygro(+). The plasmid p916B2L was constructed by inserting the *NheI*-*XbaI* fragment, which contained the signal peptide region from pLL-B404 to producing the light chain of MAb B404 (Kuwata et al., 2011) and the light chain λ gene from MAb 916B2, into pcDNA3.1/Hygro(+). Plasmids, plgG, pCOMB3XSS and pCOMB3XTT were kindly provided from Dr. Barbas (The Scripps Research Institute).

Recombinant antibodies were obtained by co-transfection of heavy and light chain plasmids to 293A cells (Life Technologies, Carlsbad, CA) and cells stably expressing antibodies were selected with G418 (800 µg/ml) and Hygromycin (160 µg/ml). The nucleotide sequence of MAbs was determined using a Big Dye Terminator, version 1.1 (Applied Biosystems, Life Technologies, Carlsbad, CA) and the genetic analyzer A&B 3500/3500xL (Applied Biosystems, Life Technologies, Carlsbad, CA). Sequences were aligned and analyzed using the CLC Sequence viewer 6 (CLCbio, Boston, MA). Evolutionary analyses were conducted in MEGA5 (Tamura et al., 2011).

Binding activity of MAbs to HIV-1 Env by ELISA analysis

Capture ELISA described in the previous section and Flow cytometry were used to determine the binding of the MAbs to